JOURNAL OF

THE ROYAL SOCIETY OF WESTERN AUSTRALIA

Volume 72 • Part 3 • 1990

ISSN 0035-922X

The Royal Society of Western Australia

To promote and foster science in Western Australia
and counteract the effects of specialization

PATRON

Her Majesty the Queen

VICE-PATRON

His Excellency the Governor
of Western Australia

COUNCIL 1989-90

President	M Candy BSc MSc FRAS
Vice-President	B Dell BSc (Hons) PhD
	K McNamara BSc (Hons) PhD
Past President	J S Pate PhD DSc FAA FRS
Joint Hon Secretaries	J R Gozzard BSc (Hons)
	W A Cowling B Agric Sc (Hons) PhD
	L N Thomas BSc MSc
Hon Treasurer	J Dodd BA MSc PhD
Hon Librarian	M A Triffitt BA ALAA
Hon Editor	I Abbott BSc (Hons) PhD
Hon Journal Manager	P Birch BSc Dip Comp
Members	L E Koch BSc MSc PhD
	J S Beard BSc MA D Phil
	V Semeniuk BSc (Hons) PhD
	P Playford BSc PhD
	J Fox BSc MSS MSc PhD
	D Walker BSc D Phil

Journal of the Royal Society of Western Australia 72 (3), 1990, 63-66

Mortality and growth of tree species under stress at Lake Toolibin in the Western Australian Wheatbelt

David T Bell & Raymond H Froend

Department of Botany, The University of Western Australia
Nedlands WA 6009

Manuscript received June 1988; accepted December 1988

Abstract

Tree species occupying the bed and margins of Lake Toolibin, an ephemeral lake of the Northern Arthur River system in the central Western Australian Wheatbelt, were permanently marked in 1983 and then remeasured after 5 years to determined survival, growth and vigour. Trees of the lake margins, *Eucalyptus rudis* and *Melaleuca strobophylla*, showed the greatest mortality, greatest reduction in vigour classification and smallest growth increments to the environmental conditions of the lake now being affected by secondary salinisation. The upland species, *Acacia acuminata* and *Allocasuarina huegeliana*, also showed elevated levels of mortality and reduced vigour, but had the highest annual growth increments of the species measured. *Casuarina obesa* populations in the more saline areas of the lake environment showed increased mortalities, decreased vigour and reduced growth compared to the trees of areas of the lake environment with more favourable conditions.

Introduction

Lake Toolibin (32°56'S, 117°11'E) is one of the few comparatively fresh water lakes in the central Western Australian Wheatbelt and one of particular importance as a waterfowl breeding location. The lake lies at the head of the chain of shallow ephemeral lakes of the Northern Arthur River, a tributary of the Blackwood River System, in the Wickepin Shire. All other lakes of the Arthur River System have been severely affected by secondary salinization and the Shire has lost more than 3% of its formerly arable land to the effects of increased salinity and flooding (NARWRC 1978).

Lake Toolibin and its surrounds, incorporated in Reserves 27286 and 9617, have been intensively monitored since the impacts of secondary salinization were first noticed in the early 1970s (NARWRC 1978). Currently the Department of Conservation and Land Management is engaged in a tree planting and groundwater pumping operation to restrict the further decline of this important region of indigenous flora and fauna.

Detailed mapping of topographical, environmental and vegetational features revealed patterns of plant community distribution and relative health and vigour of the communities in relation to the input of salinity from the several drainage systems (Froend *et al* 1987). *Casuarina obesa* dominates the seasonally inundated lake bed. *Melaleuca strobophylla* occurs on slightly raised sections of the lake floor and *Eucalyptus rudis* can be found along the margins of the lake and inlet drains. Upland areas around the lake are dominated by open woodlands of *Eucalyptus loxophleba*, *Allocasuarina huegeliana* and *Acacia acuminata*.

Study of the patterns of tree deaths in the lake environment has indicated that the increasing salinity levels have adversely affected the populations of *Casuarina obesa* and *Melaleuca strobophylla* while both increased salinity and prolonged inundation have affected *Eucalyptus rudis* (Froend *et al* 1987). The current study reports on the mortality, change in tree vigour and incremental growth achieved in permanently marked populations from 1983 to 1988.

Methods

Five study areas were established during the Autumn of 1983 in and around Lake Toolibin. All trees were tagged at breast height with a permanent aluminium tag, mapped, measured for diameter and subjectively scored for vigour (0 = healthy to 9 = dead). The elevation of each tree in relation to lake levels was determined in Autumn, 1983.

Although it is realized that soil salinity levels vary greatly with season, the 1983 data on the percentage of the dry soil weight as NaCl contribute some indication of the severity of each study area (Table 1).

Table 1

Features of the tagged tree plots (After Froend *et al* 1987).

Area 1 A transect of four plots (each c. 20m X 20m) grading from the western upland of the Northern Arthur River channel dominated by *Eucalyptus loxophleba* across the *Casuarina obesa* - dominated floodplain and up into the eastern upland woodland. All elevation are above mean lake level. Salinity levels in March 1983 ranged between 0.04 % NaCl in the uplands to 0.13 % in the heavy soils near the channel margin.

Area 2 A transect of 3 plots grading from upland *E. loxophleba* - *Acacia acuminata* woodland into the lake basin region dominated by *Casuarina obesa* on the eastern margin of the lake where water conditions tended to be fresher. Salt concentrations in the upland were low, at 0.04 % NaCl. Some lake bed sections in this area reached 0.12% NaCl in March 1983.

Area 3 A location of 4 plots on the western edge of the lake just south of the Western Drain, the source of a major input of salts and the major region of tree damage in 1983. Upper reaches are dominated by *Eucalyptus rudis* with *Casuarina obesa* and *Melaleuca strobophylla* in the lake bed portions of the area. Mean soil salinity levels reached 0.30 % NaCl.

Area 4 A relatively flat region in the central part of the lake basin harbouring a monoculture stand of *Casuarina obesa* some 300 m east of Site 3. The two plots had a mean soil salinity of about 0.07% NaCl. Inundation percentages were the highest of the study sites due the central basin location.

Area 5 A single plot site located in the Northwest Creek drainage, an area of moderate input of salinity. This plot was not analysed for soil salinities in 1983. The major species of the lowlying area was *Casuarina obesa* with *E. rudis* in marginally higher sections of the area.

In May 1988, all trees were remeasured for diameter at breast height with diameter tapes and again scored for vigour class. The permanent tag at breast height ensured that the measurements were taken at the same circumference of the tree as previously. The percentage mortality of trees and change in diameter and vigour for all species, except *Casuarina obesa*, were determined by combining the data for all sites. Sufficient numbers of *Casuarina obesa* allowed comparisons of the several locations within the lake environment on the mortality, vigour and growth.

Results

The two common lake bed/lake margin species, *Melaleuca strobophylla* and *Eucalyptus rudis*, showed relatively high mortality rates with nearly a quarter of the tagged trees dying in the 1983-1988 period (Table 2). Mortality was also relatively high in the upland species *Acacia acuminata* and *Allocasuarina huegeliana*, however, mortality was nil in *Eucalyptus loxophleba*. Change in vigour class mirrored the mortality percentages with *Melaleuca strobophylla* showing the greatest mean change in vigour and *Eucalyptus loxophleba* showing the least change in vigour over the five year period. The separate population calculations of mortality, vigour and growth in *Casuarina obesa* revealed that mortality was highest at the midlake region (area 4), but in general most trees tagged in 1983 survived until the resample period of 1988 (Table 3). Trees of the lake bottom near the eastern perimeter at area 2 showed the greatest change in vigour, a reduction of more than 4 units in the 5 years. Total growth increment was smallest in the trees of the midlake site (area 4) and the lake bottom trees growing on the western edge of the lake (area 2), but the growth rates of *Casuarina obesa* at some of the other sites were comparable to those tree species growing in the apparently more favourable habitats above the lake margin.

Table 2

Percentage mortality, change in vigour class and increment growth of tree species of Lake Toolibin, Western Australia

Values are means ± standard deviations. The annual increment was determined as one-fifth of the 5 year change in diameter

Species	N	Mortality %	Change in Vigour	Growth Increment (cm) 1983-1988	Annual
Acacia acuminata	14	21	-2.0 ± 1.8	2.34 ± 2.09	0.47
Allocasuarina huegeliana	8	25	-1.7 ± 1.4	1.90 ± 2.16	0.38
Eucalyptus loxophleba	14	0	-0.7 ± 0.7	1.02 ± 0.75	0.20
E. rudis	16	25	-1.7 ± 2.7	0.32 ± 1.00	0.06
Melaleuca strobophylla	15	27	-4.4 ± 2.7	0.47 ± 1.07	0.09

Table 3

Percentage mortality, change in vigour class and increment growth (± sd) of *Casuarina obesa* populations growing on the bed of Lake Toolibin, Western Australia

Area	N	Mortality %	Change in Vigour	Growth Increment (cm) 1983-1988	Annual
1	39	10	-2.0 ± 1.7	1.26 ± 1.14	0.25
2	22	0	-3.7 ± 4.0	0.80 ± 0.91	0.16
3	23	4	-0.2 ± 1.7	1.34 ± 1.06	0.27
4	87	17	-1.6 ± 1.3	0.44 ± 0.44	0.09
5	17	0	-0.8 ± 0.8	1.44 ± 0.62	0.29

Discussion

Species commonly occupying regions of annual flooding have a high tolerance of saturated soil conditions (Pereira & Kozlowski 1977) and often can tolerate considerable increase in flooding duration before death occurs (Green 1947). Several years of permanent inundation are required to cause death in such species (Yeager 1949, Eggler & Moore 1961).

The tolerance of river bottom or ephemeral lake species to the combined stresses of increased flooding durations and increased salinity, however, has not been previously recorded. Australia is somewhat unique in that the clearing of large tracts of woodland is now resulting in the combined stresses of increased waterlogging durations and higher levels of soil salinity occurring in catchment discharge areas (Nulsen 1986). The response of the vegetation in the Lake Toolibin region to secondary salinization seems to have been one of greater effect on the lake margin species than those inhabiting the environments of the lake bottom or the upland regions unaffected by inundation. *Casuarina obesa* has been shown to be highly tolerant of salinity and waterlogging stresses (van der Moezel *et al* 1988). Although areas of high *C. obesa* mortality exist, over the majority of the lake bed the increase in stress apparently still lies within the limits of tolerance for the mature *C. obesa* trees. In *Melaleuca strobophylla* and *Eucalyptus rudis*, however, the longer periods of saturated soil profiles induced by the clearing of upland recharge zones of the catchments and the increased levels of groundwater salinity have combined to stress individuals of these two species to the point of mortality. *Eucalyptus rudis* has been previously shown to be adversely affected by increasing periods of soil saturation (Froend *et al* 1987). Certain species of *Melaleuca*, for example, *M. acacioides* (Barlow 1986) and *M. styphelioides* (Midgley *et al* 1986), show tolerance to soil salinity, but no studies on *M. strobophylla* have been carried out to indicate suspected abilities to tolerate increasing levels of flooding conditions or groundwater salinity. The present study indicates that these species appear sensitive to secondary salinization and require careful monitoring in the future for further degradation of stream courses in the central Wheatbelt.

The mortality of the upland species is more difficult to explain. Remnant woodlots in rural areas of Australia have reputedly suffered large tree population losses since the late 1960s and early 1970s. This decline in rural tree populations is probably due to several reasons. The first, loss due to removal of trees as part of farm management, and the second, due to old age, coupled with a paucity of recruitment of tree seedlings because of active suppression, grazing and competition with improved pastures, are easily understood reasons for rural tree population decline. In the present study deaths in *Acacia acuminata*, *Allocasuarina huegeliana* and *Eucalyptus rudis* occurred in reasonably large trees but it would be difficult to conclude that all deaths were due to old age. A third element, "rural dieback", the premature and relatively rapid decline and death of native trees on farms, is apparently a consequence of interacting environmental stresses and remains largely unexplained (Old *et al* 1981). It is apparent, however, that remnant woodlands in rural landscapes represent ecosystems which are precariously balanced (Wylie & Landsberg 1987). Rural woodlands have little chance of survival unless supplemented by replanting or by natural regeneration. The data of the present study further document this phenomenon, but provide no clues to its cause.

The efforts of the Department of Conservation and Land Management to reafforest the upland margins of the Lake Toolibin reserves and the pumping of saline groundwaters from the lake basin environment should provide a more favourable habitat for the present population of trees and encourage natural recruitment. The Lake Toolibin reserves would be a logical location to establish a more extensive series of plots to study seedling recruitment and mortality and crown condition by age class of each major species of the area. Hopefully the patterns of poor survival, decline in vigour and slow growth rates recorded during the past five year period will be reversed in the future.

References

Barlow B A 1986 Contributions to a revision of *Melaleuca* (Myrtaceae) 1-3 Brunonia 9:163-177.

Eggler W A & Moore W B 1961 The vegetation of Lake Chicot, Louisiana, after eighteen years of impoundment. Southwest Nat 6 175-183

Froend R H, Heddle E M, Bell D T & McComb A J 1987 Effects of salinity and waterlogging on the vegetation of Lake Toolibin, Western Australia Aust J Ecol 12:281-298.

Green W E 1947 Effects of water impoundment on tree mortality and growth. J For 45 118-120.

Midgley S J, Turnbull J W & Hartney V J 1986 Fuel-wood species for salt affected sites. Reclam Reveg Res 5:285-303

Northern Arthur River Wetlands Rehabilitation Committee (NARWRC) 1978 Progress Report. Unpublished report to the State Minister of Fisheries and Wildlife

Nulsen R A 1986 Management to improve production from salt affected soils. Reclam Reveg Res 5:197-209

Old K M, Kile G A & Ohmart C P 1981 Eucalypt Dieback in Forests and Woodlands. CSIRO, Melbourne

Pereira J S & Kozlowski J T 1977 Variations amongst woody angiosperms in relation to flooding. Physiol Plant 41 184-192.

van der Moezel P G, Watson L E, Pearce-Pinto G V N & Bell D T 1988 The response of six *Eucalyptus* species and *Casuarina obesa* to the combined effect of salinity and waterlogging Aust J Plant Physiol 15 465-474

Wylie J R & Landsberg J 1987 The impact of tree decline on remnant woodlots on farms In 'Nature Conservation: The Role of Remnants of Native Vegetation (eds D A Saunders, G W Arnold, A A Burbidge & A J M Hopkins) Surrey Beatty & Sons, Chipping Norton, New South Wales, 331-332

Yeager L L 1949 Effect of permanent flooding in a river-bottom timber area Bull Illinois Natur Hist Surv 25,33-65.

Journal of the Royal Society of Western Australia 72 (3), 1990, 67-74

Motor vehicle emission inventory for the Perth airshed

T J Lyons, R O Pitts, J A Blockley,
J R Kenworthy & P W G Newman

Environmental Science,
School of Biological and Environmental Sciences,
Murdoch University, Murdoch WA 6150

Manuscript received July 1988; accepted December 1988

Abstract

A motor vehicle emission inventory is developed for the Perth metropolitan airshed by integrating data on traffic flow conditions with emission factors that incorporate the effects of both speed and acceleration. This highlights the impact of varying driving conditions on the spatial and temporal resolution of vehicle emissions, and illustrates that traffic congestion enhances pollutant production through increased variations in vehicle accelerations

Introduction

Air quality within Perth is for most days of the year exceptionally clean when compared to cities of comparable size (Bottomley & Cattell 1974, Lax *et al* 1986). However under suitable meteorological conditions pollution events can occur that exceed the USA primary and secondary standards (Bottomley & Cattell 1974, KAMS 1982). These are generally associated with light stable synoptic pressure gradients (Bottomley & Cattell 1974) or mesoscale phenomena, such as the sea breeze (KAMS 1982)

With Perth, the emission of gaseous pollutants is confined to two major sources: an industrial area concentrated to the southwest of the metropolitan area and motor vehicles within the region (Lax *et al* 1986). The Kwinana industrial area emits large quantities of SO_2 and to a lesser extent NO_x (KAMS 1982). These emissions have been modelled under both stable conditions (Kamst & Lyons 1982) and sea breeze fumigation (KAMS 1982), as well as in a standard climatological model based on Gaussian techniques (KAMS 1982). In all cases, the models applied to the immediate region surrounding Kwinana and did not attempt to incorporate the broader airshed concept.

An analysis of the air quality across the broader metropolitan airshed requires the estimation of the other major source outside the industrial area, motor vehicles. These are the source of oxides of nitrogen (NO_x), brake lining dust, hydrocarbons (HC), carbon monoxide (CO), smoke, aldehydes, lead salts and particles, rubber, gaseous petrol and carbon particles (Lay 1984). All of the CO and NO_x are emitted from the exhaust pipe whereas approximately 50% of the HC's from an uncontrolled vehicle are emitted via the exhaust, with the remainder coming from the crankcase, carburetor and fuel tank vents (SPCC 1980).

Evaporative emissions result from the fuel system leaking HC's to the atmosphere at a rate determined by the temperature of the system (diurnal emissions) and hot soak emissions occuring after the vehicle has been driven some distance, through heating of the carburetor and fuel lines (Nelson 1981). Hamilton *et al* (1982) estimated evaporative emissions from typical early 1970's vehicles as 0.8 g km^{-1} and noted that these are generally constant through the life of the vehicle. Subsequent to 1975, Australian emission standards (Table 1) have resulted in improved pollution control, as evidenced by Nelson (1981). He confirmed diurnal evaporative emission factors of 22.1 g $vehicle^{-1}$ day^{-1} for uncontrolled (pre 1975), and 5.1 g $vehicle^{-1}$ day^{-1} for controlled vehicles, respectively, with hot soak emissions of 12.5 g $vehicle^{-1}$ for uncontrolled, and 4.2 g $vehicle^{-1}$ for controlled vehicles. Consequently, evaporative emissions are a function of the age of the fleet whereas exhaust emissions are also dependent on vehicle driving characteristics. Hence the spatial and temporal variation of emission source strength is dependant on driving chracteristics across the airshed as well as the age mix of the fleet.

Table 1

Australian emission standards, g km^{-1}. (after SPCC 1980)

	Date of Manufacture	
	After 1 July 1976	After 1 January 1981
CO	24.2	18.6
HC	2.1	1.75
NO_x	1.9	1.9

Vehicle emissions in Sydney were estimated by Stewart *et al* 1982 from the product of vehicle kilometres travelled (VKT), emissions per kilometre for each model year and travel fraction done by each model year. Although this gives a bulk estimate across the airshed it does not allow for the spatial resolution of the sources nor does it account for variations in driving conditions.

From a preliminary dynamometer test of 28 vehicles, Kent & Mudford (1979) found that typical emissions under Australian urban driving conditions, at that time, could be expressed as:

$$[CO] = 465s^{-0.97}$$
$$[HC] = 21.5s^{-0.73}$$
$$[NO_x] = 2.2 + 0.008s$$

where [CO] is the carbon monoxide emission (g km $^{-1}$), [HC] hydrocarbon emission (g km $^{-1}$), [NO_x] oxides of nitrogen emission (g km $^{-1}$) and s the average vehicle speed (km h^{-1}). These are of a similar form to the estimates used by Iverach *et al* (1976), based on US experience, and equivalent to the values employed by Taylor & Anderson (1982).

Such an estimation assumes emissions can be represented in terms of average speed alone and neglects the influence of variations in driving conditions, particularly changes in acceleration, on emissions. For example, Kent & Mudford (1979) found that a three dimensional plot of emission rates against speed and acceleration led to parabolic surfaces for CO and HC's, while NO_x showed a general increase in emission rates with speed and acceleration. In particular, they found that both CO and NO_x show marked increases in emission rate with positive acceleration. This cannot be accounted for from an average speed model and highlights the need to incorporate a wide range of accelerations and speeds to produce reasonably representative emission inventories.

Thus the spatial resolution of these emissions requires an integration of data concerning traffic flow characteristics with data on vehicle numbers, vehicle types and VKT. Previous work in this area has emphasized the latter data on vehicles and has lacked any detailed input about how those vehicles are being driven (SATS 1974, Visalli 1981). A very basic approach to incorporate driving patterns has been attempted for Melbourne but uses only the standard Los Angeles driving cycle for its traffic characteristics (Neylon & Collins 1982).

Hence this paper addresses the development of a motor vehicle emissions inventory for the Perth urban area based on actual driving pattern data across the urban area as well as vehicle emission data resolved on the basis of speed and acceleration. Pollutant source strengths are expressed as the total emission averaged over a specified time period and a specified grid square of the airshed.

Methodology

Kenworthy *et al* (1983) used an urban ecological approach in treating the city as an integrated system, to obtain representative driving cycles across Perth. They div-

Table 2

A summary description of the six driving pattern areas in terms of the major factors used to derive them (after Kenworthy *et al* 1983). Note all rankings of characteristics are made relative to the mean of Perth.

Characteristics / Area	Social Economic Status of Residents (Household income and vehicle ownership)	Activity Intensity of area (land use intensity, congestion, public transport availability)	Dominant modal split features of residents
Central Core Area 1	Very low	Very high	Peak periods Very low private vehicle usage, very high public transport, walking and biking
Inner suburbs Area 2	Average to low	High	All periods Very high public transport
Middle Western suburbs Area 3	Average to high	Average to high	Off peak Very low public transport usage
Middle South, outer North and Eastern suburbs Area 4	High	Low	Peak periods High private vehicle usage, low public transport, walking and biking
Outer South East and North East suburbs Area 5	Average	Very low	Off peak Very high private vehicle usage, very low walking and biking
Northern State Housing suburbs Area 6	Low	Average to low	Off peak Very low private vehicle usage, very high walking and biking

ided the metropolitan area into six regions characterized in terms of socio-economic status and activity intensity (Table 2), and using the chase car technique (Scott Research Laboratories 1971) obtained detailed second by second speed time histories of typical urban driving in each of these regions. Although statistically representative driving cycles can be generated from such data, they suffer a considerable loss in speed resolution (Lyons *et al* (1986). Hence, Kenworthy *et al* (1983) obtained representative driving cycles for each region by matching summary characteristics to the observed speed time traces, which is consistent with the methodology adopted by Kuhler & Karstens (1978). Accordingly, they obtained the representative urban driving speed time traces summarized in Table 3, for morning peak (MP), evening peak (EP) and off peak (OP) periods for each region.

These speed time traces were converted into speed acceleration probability matrices, where each matrix cell, of size 5 km h^{-1} by 1 km h^{-1} s^{-1}, contains the total number of one-second observations in the respective range from the representative driving cycle. Thus each matrix element represents the total time during the representative driving cycle that the vehicle was at that speed and acceleration.

Post *et al* (1985) extended the analysis of Kent & Mudford (1979) to 177 Australian light duty vehicles in use, and obtained fleet averaged emission rates as a function of vehicle velocity and acceleration. Their results are presented at the same resolution as the speed acceleration probability matrices. Since cell averaged emission rates are independent of the velocity profile followed by the vehicle (Post *et al* 1981a,b), these can be used to estimate emissions for any driving pattern, assuming that the vehicles used by Post *et al* (1985) are representative of the typical Australian urban fleet. Hence the total emissions over a representative driving cycle can be expressed as

$$[P] = \sum_{i=1}^{n} \sum_{j=1}^{n} e_{i,j} \; t_{i,j}$$

where [P] is the emission (g) of pollutant species P, $e_{i,j}$ is the emission rate (g s^{-1}) of pollutant species P for the matrix element defined by velocity i and acceleration j (Post *et al* 1985), t_{ij} total time(s) vehicle spent at that velocity and acceleration during the driving cycle and the summation is over all possible speed acceleration cells. [P] is the total emission over the period of the driving cycle. Hence the characteristic emission factor (g km^{-1}) for that driving cycle can be represented as

$$[P]_k = [P] / d_k$$

where d_k is the distance covered during the driving cycle (see Table 3).

Table 3

Characteristics of representative driving cycles for each area and time period, where MP is morning peak, OP off peak and EP evening peak

Area		Dist. from CBD (km)	Aver. Speed (km h^{-1})	RMS Accel. (m s^{-2})	Stops per km. (km^{-1})	Idle Time (%)	Cruise Time (%)	Distance d_k (km)
1		2						
	MP		30.0	0.89	1.60	20.6	13.8	11.9
	OP		35.1	0.86	1.43	15.6	13.7	11.9
	EP		30.6	0.87	1.60	18.4	12.5	11.9
2		5						
	MP		36.4	0.80	1.39	17.9	27.5	14.5
	OP		43.1	0.82	0.84	9.6	38.3	14.2
	EP		38.8	0.85	0.95	17.9	30.3	16.8
3		9						
	MP		40.6	0.78	0.79	11.4	30.8	17.7
	OP		46.7	0.70	0.45	5.3	35.5	17.8
	EP		45.3	0.71	0.56	8.2	38.5	17.7
6		11						
	MP		42.4	0.74	0.72	13.3	36.7	19.4
	OP		47.4	0.76	0.54	11.3	44.7	20.3
	EP		45.2	0.76	0.64	14.4	49.5	20.3
4		13						
	MP		37.6	0.77	1.08	14.3	30.6	19.4
	OP		46.8	0.80	0.67	10.1	46.7	19.4
	EP		41.1	0.76	0.82	18.3	33.7	19.4
5		19						
	MP		52.9	0.69	0.33	3.4	59.4	18.4
	OP		52.0	0.70	0.27	3.6	55.2	18.3
	EP		50.0	0.78	0.30	4.6	54.9	19.8

Within Australia, exhaust emission rates for CO and NO_x for heavy duty diesel powered vehicles remain uncontrolled and no locally validated data was readily available. Emission rates based on US experience and assumed independent of vehicle speed are listed in Table 4 (Stern 1976, USEPA 1977). These represent uncontrolled emissions averaged over a number of vehicles, operating under a variety of conditions, and are consistent with the heavy duty emission rates used by Jakeman *et al* (1984) for Australian conditions. Luria *et al* (1984) obtained similar values for buses and expressed the emission factors for NO_x, HC and CO as a function of speed. They showed a marked decrease in CO and HC emissions with speed and an increase in NO_x emissions up to a speed of 40 km h^{-1}. In the absence of alternate emission factors these were used.

Trucks within the Perth metropolitan area are mostly able to maintain easy cruise conditions and appear to avoid built up areas and peak conditions (Lyons *et al* 1987). Unlike automobiles, their driving cycle shows no dependence on location or time period. Consequently, as the heavy duty diesel emission factors are only expressed as a function of speed, the average speed from the Perth truck driving cycle of 43.2 km h^{-1} (Lyons *et al* 1987) was assumed for all truck emissions, leading to the emission factors shown in Table 4.

Table 4

General emission factors (g km^{-1}) for heavy duty diesel powered vehicles (after [1]Stern 1976; [2]USEPA 1977) and those used in this study assuming an average speed of 42.3 km h^{-1} (after [3]Luria *et al* 1984).

Pollutant	Emission factor g km^{-1} (1, 2)	(3)
Particulates	0.8	
CO	17.8	9.5
HC	2.9	1.5
NO_x	13.0	10.2
Aldehydes	0.2	
Organic acids	0.2	
SO_x	1.7	

The total emission in any period and any area of the city can be expressed as

$$E = \sum_{m=1}^{m=n} [P]_{k,m} \, VKT_{k,m}$$

where $[P]_{k,m}$ and $VKT_{k,m}$ are the emission factor and total VKT, respectively, for that time period and area and the summation is over vehicle type.

Results and Discussion

Combining the characteristic driving patterns (Kenworthy *et al* 1983) and the fleet emissions (Post *et al* 1985) led to the automobile emission factors shown in Table 5 for each of the representative areas. As these factors are based on the same fleet data, the differences are directly attributable to the style of driving in each of the areas. This emphasizes the contribution of variations in speed and acceleration patterns across a metropolitan area in determining the spatial variation of emissions.

Table 5

Emission factors g km^{-1} for exhaust emissions for each time period and region based on speed acceleration matrix.

Area	1	2	3	6	4	5
NO_x						
MP	1.9	1.8	1.8	1.7	1.9	1.7
OP	1.9	1.9	1.7	1.8	2.0	1.7
EP	1.8	1.8	1.8	1.9	1.9	1.8
CO						
MP	21.8	18.4	18.1	16.9	19.2	14.8
OP	19.2	17.4	15.7	15.9	16.8	15.2
EP	21.3	18.5	16.7	16.9	17.5	16.0
HC						
MP	2.2	1.9	1.9	1.8	2.0	1.8
OP	2.0	1.8	1.7	1.8	1.8	1.7
EP	2.2	1.9	1.8	1.9	1.8	1.7

The corresponding automobile emission factors based solely on average speed in each of the regions (Table 3) are shown in Table 6. With the exception of the NO_x emission factors, the average speed factors are lower, as would be expected, since the incorporation of acceleration leads to greater variability in the driving patterns and hence higher emissions. The NO_x emissions are higher because the average speed equation implies a speed independent emission of 2.2 g km^{-1} (Kent & Mudford 1979) compared to the idle emission of 0.039 g min^{-1} of Post *et al* (1985). Their results also suggest that emissions of the order of 2.2 g km^{-1} are only observed under high acceleration which is not maintained for any length of time in representative urban driving cycles (Lyons *et al* 1986).

Table 6

Emission factors (g km^{-1}) for exhaust emissions for each time period and region based on average speed.

Area	1	2	3	6	4	5
NO_x						
MP	2.4	2.5	2.5	2.5	2.5	2.6
OP	2.5	2.5	2.6	2.6	2.6	2.6
EP	2.4	2.5	2.6	2.6	2.5	2.6
CO						
MP	17.2	14.2	12.8	12.3	13.8	9.9
OP	14.7	12.1	11.2	11.0	11.2	10.1
EP	16.8	13.4	11.5	11.5	12.7	10.5
HC						
MP	1.8	1.6	1.4	1.4	1.5	1.2
OP	1.6	1.4	1.3	1.3	1.3	1.2
EP	1.8	1.5	1.3	1.3	1.4	1.2

Within Perth, areas 1 and 5 illustrate the greatest differences in activity intensity ranging from the congested CBD, with its greater reliance on public transport, to the private vehicle dominated outer suburbs. Emission factors, based on the speed/acceleration distribution, show a decrease in emission factor between the CBD and the outer suburbs for NO_x corresponding to decreased accelerations characterised by high average speeds and maintained cruise conditions. Alternatively, emission factors based solely on average speed illustrate an increase as you move away from the congested CBD. Thus, a simple average speed model suggests higher emissions away from the congested CBD by not accounting for the marked acceleration changes induced by the congested stop start driving of the CBD.

The Perth metropolitan region was divided into grid squares of 1 km by 1 km and estimated daily VKT for each of these was obtained from traffic count information collected by the Main Roads Department (MRD 1986). Automatic traffic counts, of 1-3 days duration, are carried out on all major roads in the region, as well as points on these at which a change in volume might be expected. They are expressed as annual average weekday traffic flow and represent the 24 hour traffic volume passing through a site on a typical weekday (MRD 1986).

These individual grid values were summed to provide an overall measure of the recorded total daily VKT for Perth. Any shortfall between this figure and the estimated total VKT, listed in Table 7, can be attributed to subarterial roads. This was allocated across the region on the basis of the recorded traffic volumes.

24 hour VKT weightings for Perth are 16.5% morning peak (0700-0900), 18.5% evening peak (1600-1800) and 65% for all off-peak times (Kenworthy *et al* 1983). Consequently, the daily VKT for each grid square was corrected by these factors and divided by the length of the period to provide an hourly estimate of non-truck VKT.

The truck and non-truck VKT were then multiplied by the appropriate emission factors (Tables 4, 5), to provide an estimate of the total vehicle exhaust emission across the metropolitan area. Additional evaporative emissions are accounted for from the distribution of registered vehicles and added to the total for HC. Figure 1 illustrates the spatial variation of the calculated morning peak and off peak NO_x emissions. The major arterial roads are clearly visible as well as the increased emission during the morning peak period. Given the small variation in NO_x emission factors across the region, the major spatial variations are the direct result of variations in VKT. Similar maps were obtained for the other pollutant species.

Emission totals presented in Figure 1 are not directly verifiable as they are based on average traffic conditions across the metropolitan area, which are not necessarily observed on any one day. However they do indicate the spatial variation in source strength and provide an indication of the relative magnitude of pollutant sources in different regions. An alternative statistic can be obtained from Table 5 by computing the predicted CO/NO_x ratio on the basis of both time period and location (Table 8).

Table 7

Estimated total VKT (Vehicle Kilometres Travelled) for Perth for 1985. Note weekend VKT is estimated at 1.5 average weekday VKT (after ABS 1985).

Vehicle Class	Total Annual VKT (10^9 km)	Equivalent average daily VKT (10^7 km)
Automobiles	6.996	2.064
Utilities/Panel vans	1.168	0.345
Total Motor vehicles	8.164	2.409
Trucks	0.445	0.131
Motor cycles	0.138	0.041
Total	8.747	2.581

The total truck VKT, given in Table 7, was allocated to high truck usage routes in the metropolitan area (Lyons *et al* 1987) on the basis of the total grid VKT and subtracted from the individual grid totals. As the truck driving cycle is independent of peak periods, the truck VKT was divided by 24 to represent an average hourly truck VKT.

Table 8

Variation of CO/NO_x ratio across the Perth airshed resulting from temporal and spatial variation in driving patterns, where MP is morning peak, EP evening peak and OP off peak.

Region	CO/NO_x ratio MP 0700-0900	EP 1600-1800	OP
1. Central Core	11.5	11.8	10.1
2. Inner suburbs	10.2	10.3	9.2
3. Middle western suburbs	10.1	9.3	9.2
4. Middle south, outer north and eastern suburbs	9.9	8.9	8.8
5. Outer south east and north east suburbs	10.1	9.2	8.4
6. Northern state housing suburbs	8.7	8.9	8.9

The greater congestion and higher accelerations as you approach the CBD leads to an increase in the CO/NO_x ratio of pollutants emitted from the exhaust pipe. As both smog-chamber and computed results suggest that added CO accelerates the depletion of NO and the generation of NO_2 as well as enhanced generation of O_3 through NO_2 photolysis (Demerjian *et al* 1974, Drake *et al* 1979), the change in driving patterns brought about by increased congestion enhances smog formation, through increased CO generation per kilometre of travel. Given the increased concentration of vehicles using the CBD this becomes significant. If evaporative emissions are also included, the greater number of vehicles in the CBD would lead to a corresponding increase in HC emissions.

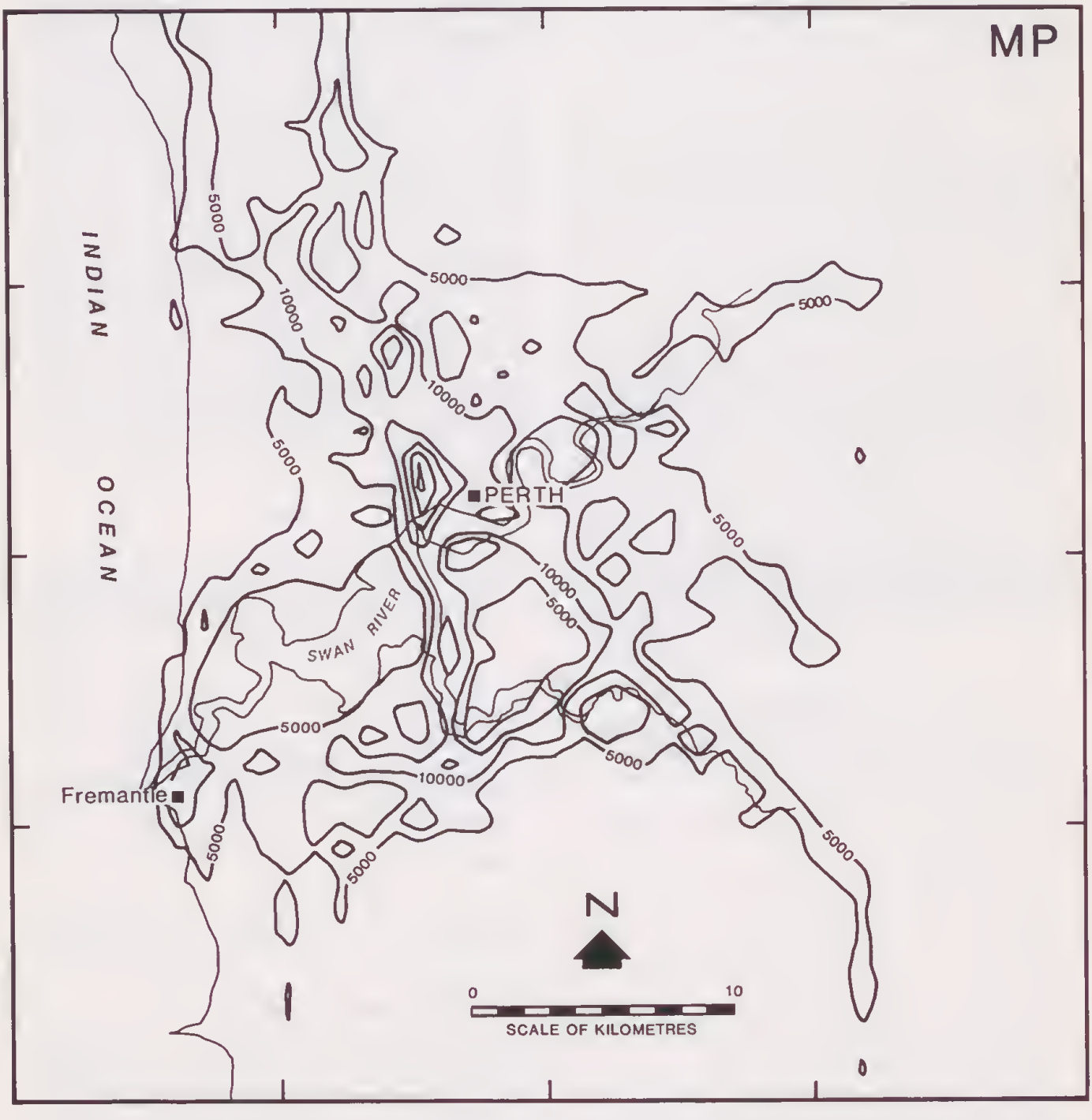

Figure 1 Predicted emission of NO_x (g hr^{-1}) across Perth for the morning peak (MP) and off peak (OP) periods.

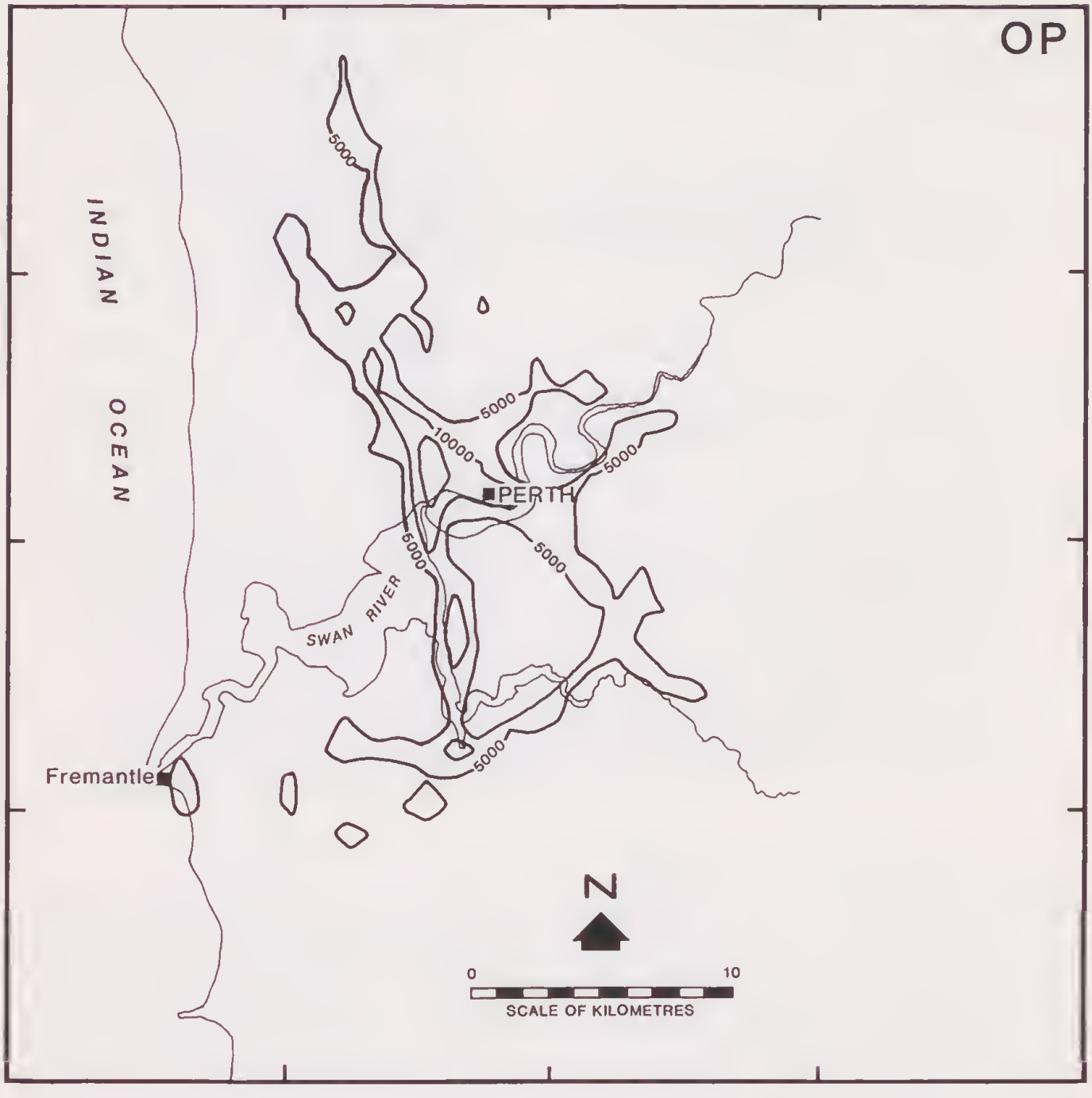

Conclusions

The integration of driving characteristics and vehicle emissions based on speed and acceleration illustrates a marked variation in emission factors from the CBD to the outer suburbs. In particular, the greater congestion and corresponding variations in acceleration within the CBD, increases the production of pollutants and the potential for photochemical smog through enhanced CO production.

Acknowledgements The development of the Perth airshed model has been funded under the Australian Research Grants Scheme, whereas the driving cycle data was collected under funding from the State Energy Commission of Western Australia and the National Energy Research, Development and Demonstration Programme, which is administered by the Commonwealth Department of Resources and Energy. All of this assistance is gratefully acknowledged.

References

ABS 1985 Survey Motor Vehicle Usage for 12 months ended 30 September 1985. Australian Bureau of Statistics.

Bottomley G A & Cattell F C 1974 Nitrogen oxide levels in the suburbs of Perth, Western Australia. J R Soc W Aust 58, 65-74.

Demerjian K L, Kerr J A & Calvert J G 1974 The mechanism of photochemical smog formation. Adv Env Sci Tech 4 1-262.

Drake R L, Hales J M, Mishima J & Drewes D R 1979 Mathematical models for atmospheric pollutants. Appendix B. Chemical and Physical Properties of Gases and Aerosols. EA-1131, Appendix B, Research Project 805, Electric Power Research Institute, 3412 Hillview Avenue, Palo Alto, CA 94304, USA.

Hamilton R B, Cass M R, Angus G A & Watson H C 1982 Forecasting hydrocarbon emissions from motor vehicles in the Sydney air shed. In: The urban atmosphere–Sydney, a case study (ed J N Carras & G M Johnson), CSIRO, Division of Fossil Fuels, 525-570.

Iverach D, Mongan T R, Nielsen N J & Formby J R 1976 Vehicle related air pollution in Sydney. J Air Poll Control Assoc 26: 39-44

Jakeman A J, Simpson R W & Taylor J A 1984 A simulation approach to assess air pollution from road transport. Discussion Paper, Centre for Resource and Environmental Studies, Aust Nat Univ.

KAMS 1982 The Kwinana air modelling study. WA Dept Conservation and Environment, Report 10: 1-96.

Kamst F H & Lyons T J 1982 A regional air quality model for the Kwinana industrial area of Western Australia. Atmos Environ 16: 401-412.

Kent J H & Mudford N R 1979 Motor vehicle emissions and fuel consumption modelling. Transpn Res 13A: 395-406.

Kenworthy J R, Newman P W G & Lyons T J 1983 A driving cycle for Perth. National Energy Research Development and Demonstration Council, Dept Resources and Energy, Report 79/9252: 1-326.

Kuhler M & Karstens D 1978 Improved driving cycle for testing automotive emissions. Presented Passenger Car Meeting, Troy Hilton, Troy, Michigan, June 5-9. SAE Paper 780650

Lax F, Robertson W A & Garkaklis B V 1986 Air pollution components in Perth. J R Soc W Aust 69: 19-27

Lay M G 1984 Source book for Australian roads. 2nd edition. Australian Road Research Board, 1-551

Luria M, Vinig Z & Peleg M 1984 The contribution of city buses to urban air pollution in Jerusalem, Israel. J Air Poll Control Assn 34: 828-831.

Lyons T J, Kenworthy J R, Austin P J & Newman P W G 1986 The development of a driving cycle for fuel consumption and emissions evaluation. Transpn Res-A 20A: 447-462

Lyons T J, Alimoradian B & Newman P W G 1987 A truck driving cycle for Perth. Transport Research Paper 5/87, Murdoch Univ, 1-29.

MRD 1986 Average weekday traffic flows 1980/1-1985/86 Perth metropolitan region. Main Roads Dept WA, 1-69

Nelson P F 1981 Evaporative hydrocarbon emissions from a large vehicle population. J Air Poll Control Assn 31: 1191-1193

Neylon M & Collins B 1982 Mobile source emissions inventory for the Melbourne airshed study. Proc Joint SAE-A/ARRB 2nd Conference on Traffic, Energy and Emissions, Melbourne, May 19-21, (SAE 82144).

Post K, Gibson T, Maunder A, Tomlin J, Carruthers N, Pitt D, Kent J H & Bilger R W 1981a Motor Vehicle Fuel Economy Report to NERDDC by the University of Sydney 1979-1981. Charles Kolling Research Laboratory Tech. Note ER-37, Univ Sydney

Post K, Tomlin J, Pitt D, Carruthers N, Maunder A, Gibson T, Kent J H & Bilger R W 1981b Fuel Economy and Emissions Research Annual Report by the University of Sydney for 1980-81. Charles Kolling Research Laboratory Tech. Note ER 36, Univ Sydney

Post K, Kent J H, Tomlin J & Carruthers N 1985 Vehicle characterization and fuel consumption prediction using maps and power demand models. Int J Vehicle Design 6: 72-92.

SATS 1974 Sydney area transportation study. Volume 2: Travel model development and forecasts. NSW Ministry Transport.

Scott Research Laboratories 1971 Vehicle operations Survey I and II. CRC APRAC Project No. CAPE-10-68 (1-70). PO Box 2416, San Bernardino, CA 92406, USA

SPCC 1980 Control of pollution from motor vehicles. State Pollution Control Commission, Publication MV-3, NSW Ministry for Planning and Environment, 1-24

Stern A C 1976 Air Pollution. Volume 4, Academic Press, New York.

Stewart A C, Pengilley M R, Brain R, Haley J J & Mowle M G 1982 Motor vehicle emissions into the Sydney air basin. In: The urban atmosphere-Sydney, a case study (ed J N Carras & G M Johnson), CSIRO, Division of Fossil Fuels, 485-502.

Taylor M A P & Anderson B E 1982 Modelling pollution and energy use in urban road networks. Proc 11th ARRB Conference 11 (6): 1-17.

USEPA 1977 Compilation of air pollutant emission factors. 3rd edition, USEPA, Office of Air Programs, Research Triangle Park, NC, USA, AP-42

Visalli J R 1981 Effects of variable vehicular age and classification distributions in mobile source modelling. J Air Poll Control Assn 31: 68-71.

Journal of the Royal Society of Western Australia 72 (3), 1990, 75-92

Stratification and disconformities in yellow sands of the Bassendean and Spearwood Dunes, Swan Coastal Plain, South-western Australia

D K Glassford[1] & V Semeniuk[2]

[1]33 Rockett Way, Bull Creek, WA 6155
[2]21 Glenmere Road, Warwick, WA 6024

Manuscript received September 1988; accepted January 1989

Abstract

Yellow sand of the Pleistocene Bassendean and Spearwood dunes of the Swan Coastal Plain of SW Australia contains sedimentary stratification at depth (>3-5m). Yellow sand is divided into units of high and low angled inclined strata, horizontal strata, and massive sand. Sequences of sand typically contain up to five major disconformities. Dip direction resultants of inclined strata at individual study sites indicate that Pleistocene wind directions were dominantly from the eastern sector, sub-dominantly from the NW, and to a minor extent from the W and SW. Dip direction mean vector resultant of all inclined strata is 210° indicating that the sands were transported mainly from the NE. These data preclude, as major processes, origin of the yellow sand by either *in situ* decalcification of coastal limestones or by coastal-marine derivation as carbonate-free quartz sand. Cross-strata and horizontal strata were emplaced by the migration of desert aeolian dune fields (desert ergs) during at least six glacial age arid phases, mostly during the middle Pleistocene. During the intervening wetter interglacial periods yellow sands were extensively bioturbated to depths of 3-5m, thereby degrading the dunes and producing massive yellow sand under the major disconformities.

Introduction

The Swan Coastal Plain of the Perth Basin, South-western Australia has an extensive cover of mainly Pleistocene siliciclastic sand (McArthur & Bettenay 1960, Playford *et al* 1975, 1976; Wilde & Low 1978, 1980; Fig. 1). This cover includes Bassendean Sand, yellow sand overlying Tamala Limestone, and some of their altered equivalents such as white quartz sand, brown quartz sand and brown sandstone. These sand formations traditionally have been interpreted as coastal-marine derived calcareous deposits which have been decalcified *in situ* by leaching processes to a residue of yellow quartz sand (Prider 1948, McArthur & Bettenay 1960, Lowry 1977, Wyrwoll & King 1984, amongst others).

Crucial evidence of long standing for decalcification (*eg* Prider 1948) is, that near the coast where yellow sand overlies limestone, from which traditionally it is concluded the sand was leached, the yellow sand has a massive structure (*eg* Spearwood Dunes). Inland where yellow sand does not overlie limestone it generally also has a similar massive structure (*eg* Bassendean Sand, yellow sand of the Yoganup Formation). Thus massive structure (absence of lamination/ bedding) has been cited as key evidence for an *in situ* decalcification origin. However, documentation of these sand formations in terms of their genetically important sedimentary features (*eg* stratigraphy, geometry, structure, fabric, texture and composition) is negligible.

This paper provides the first detailed treatment of primary sedimentary structures in the yellow sands of the Bassendean and Spearwood dunes within the central sector of the Swan Coastal Plain (Fig. 1). The paper deals only with Bassendean Sand and the quartz sand overlying the Tamala Limestone referred to the Karrakatta and Cottesloe soil associations (McArthur & Bettenay 1960), and specifically excludes the Cooloongup Sand with its local grey coloration and occasional shell content (Passmore 1970), yellow sand of the Yoganup Formation (Low 1971), Eaton Sand (Semeniuk 1983), the complex quartz sand deposits of the hinterland of Geographe Bay (Baxter 1977), and possible minor non-aeolian facies of the yellow sands (*eg* Wyrwoll & King 1984). It is also stressed that this study mainly concentrates on primary sedimentary features of the yellow sands and not on their pedogenic or geohydrologic alteration products such as humic quartz sand, white quartz sand and ferruginized sand. These various secondary overprints are briefly described as a background to understanding the destruction of primary sedimentary structures in yellow sands.

Previous studies

The major geological attributes of Perth Basin yellow sand have not been documented in systematic detail. These attributes should include genetically critical sedimentary features such as geomorphic expression, boundary types, stratigraphic associations and relationships, ge-

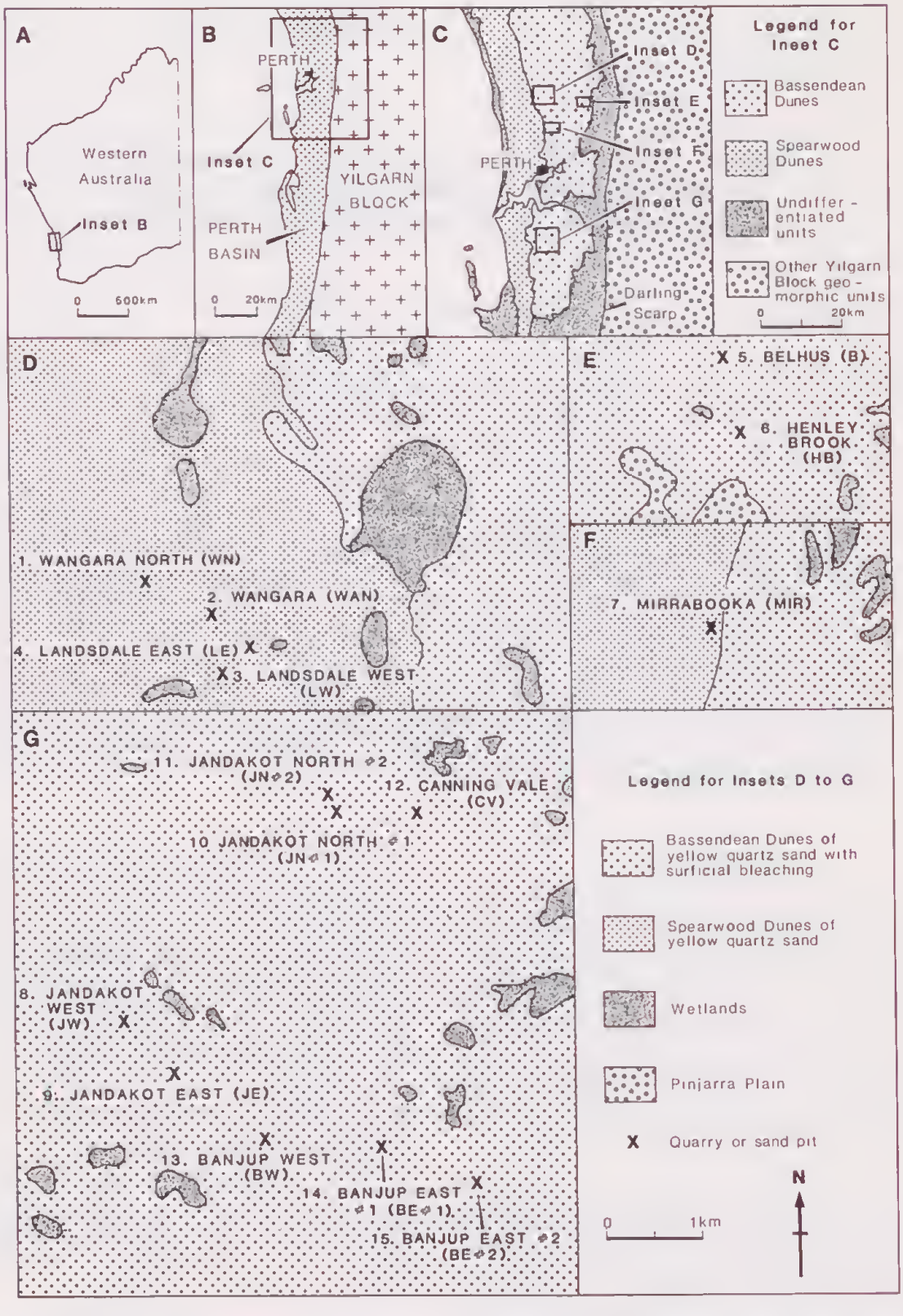

Figure 1 Location and regional setting of study sites. **A** Location of study area in Western Australia. **B** Location of study area in the Perth Basin. **C** Regional geomorphic units of the Swan Coastal Plain, the landward portion of the central Perth Basin, and their relationship to insets of study site settings (after McArthur and Bettenay 1960). **D, E, F & G** Location and setting of study sites (geomorphic unit boundaries after Gozzard 1983, 1986; Jordan 1986). Note the boundary between the Bassendean and Spearwood Dune sands as mapped by Gozzard (1983, 1986) and Jordan (1986) is 1.5 to 4km further east than it is as mapped by McArthur & Bettenay (1960).

ometry and dimensions, internal structure (types, dip angles, dip directions *etc*), fabric, texture (grain size, sorting, percentage fines, roundness, *etc*) and composition (grain types, grain coatings, internal features of grains, mineralogy of grains *etc*) (*eg* see Folk 1974, Pettijohn *et al* 1987, Lindholm 1987). Previous investigations into yellow sand have been directed towards agriculture and pedology (McArthur & Bettenay 1960), environmental and land use planning (Dept of Conserv & Envir 1980), hydrology and groundwater supply (Allen 1981), engineering (Klenowski 1976), heavy mineral deposits (Baxter 1977), geological mapping (Wilde & Low 1978, 1980; Gozzard 1983, 1986; Jordan 1986); and lithostratigraphic sub-division and definition (Low 1971, Playford & Low 1972). These studies provide information on various aspects of yellow sand, but they are not directly relevant to unravelling its origin. Despite this, many of these studies form the basis for the traditional views of coastal-marine derivation and *in situ* decalcification for the origin of yellow sand (Lowry 1977). Two published studies have dealt specifically with the genesis of Perth Basin yellow sand (Glassford & Killigrew 1976 and Wyrwoll & King 1984). These studies, however, focused mostly on the textures of yellow sand.

Although stratification is an important feature for interpreting the origin of sand (Potter & Pettijohn 1977, Lindholm 1987), it has not been the subject of any previous work on Perth Basin yellow sand. Generally, yellow sands are regarded to be structureless or massive (*eg* Prider 1948, Wyrwoll & King 1984). The only published mention, to our knowledge, of stratification in yellow sand is the reference by Baxter (1977) to "delicate cross-bedding" in Bassendean Sand in the Busselton area.

Methods

Stratification and disconformities in yellow sand sequences were studied in 15 quarry exposures in the Perth region of the Swan Coastal Plain (Fig. 1). These quarries represent all sand quarries that to our knowledge were being excavated during this study. Stratification was best studied in winter when the sand is moist. In summer, the sand is dry and commonly slumps during and following excavation. This slumping covers the deeper sequences of yellow sand, thereby typically concealing stratification. Four of the quarries are located in the middle to eastern parts of the Spearwood Dunes; eleven of the quarries are in the Bassendean Dunes. Structures within the sand were documented using the terminology of McKee & Weir (1953) and Lindholm (1987). Stratification and disconformities were mapped in the field onto panoramic photographs of quarry walls.

The true dip angle and dip direction of cross-layering was determined by measurements on partially excavated individual surfaces of the sedimentary layers or laminae of a given cross-layered set which were traceable in three dimensions. Usually 5-10 separate laminae were measured in this manner at each sampling locality. Depending on the amount of exposure, 2-5 sites typically were measured in each quarry. Dip angle and dip direction (magnetic) readings were taken according to the number and thickness of large scale cross-layered sets. Most readings were at *c* 0.5-1.5m vertical intervals for a set. For example, for a 3m thick set, three readings were taken at approximately 0.5m, 1.5m and 2.5m above the base of the set. In the case of a 5m thick set five readings were taken at approximately, 0.5m, 1.5m, 2.5m, 3.5m and 4.5m above the base of the set. The constraints of availability and wall condition of quarries has limited the data base of this paper to 228 dip angle and direction measurements of inclined strata from 12-15 localities. Additional measurements should be collected as existing quarries are excavated further and when new quarries are opened.

Sketches and photographs were used to record secondary overprints. Sediment was carefully sampled *in situ* by a 5 cm corer and retrieved to the laboratory for impregnation and slicing. Oriented thin sections were prepared from the impregnated *in situ* blocks for petrographic study. Selected laminae and groups of laminae also were sampled and sieved at half phi intervals for granulometric analysis. Representive samples and sub-samples were x-rayed with Co K-alpha radiation and diffractograms were interpreted using Brindley & Brown (1980).

Nomenclature

The Sahara Desert term erg is used in this study. Originally *erg* referred to a vast region in the Sahara Desert covered by deep aeolian sand (Gary *et al* 1972). Implicit in this original meaning were a mid-latitude location, a desert setting, and a continental, as distinct from coastal, character and derivation for the sand. Subsequent workers, however, expanded the original meaning of the term to encompass large scale coastal and non-desert aeolian sand bodies, or sand seas (*eg* Blakey *et al* 1988; Marzolf 1988). It is therefore important to define the sense in which *erg* is used. In this study *erg* refers to a vast, large scale or regional scale tract of continental desert-aeolian sand in the form of sheets and dunes. For added emphasis and clarity the term is used in conjunction with *desert*, *ie desert erg*. Other types of aeolian sand seas can then be categorized, for example, as *coastal erg* or *humid erg*.

The term *desert* is used in this paper in the sense of low to middle latitude terrains with no vegetation cover or with a vegetation cover which is too sparse to prevent widespread aeolian transport of sand. Controls such as effective rainfall, windiness, sand supply *etc* may variously contribute to producing a desert terrain. For a discussion of the main factors which can produce a desert-aeolian terrain see Ash & Wasson (1983) and Marzolf (1988).

Geological setting

The study area is within the Swan Coastal Plain, a coastal lowland of the Perth Basin with a mainly relict Pleistocene surface (Playford et *al* 1976, Wilde & Low 1978, 1980). Within this setting there is a Pleistocene lithostratigraphic unit of yellow sand (Prider 1948, Glassford 1980) relevant to this study which usually has been assigned to more than one formation (Fig. 1):

- yellow quartz sand portion of Bassendean Sand (= Bassendean Dunes of McArthur & Bettenay, 1960)
- yellow quartz sand assigned to the Tamala Limestone (within the Spearwood Dunes of McArthur & Bettenay, 1960).

To date, however, the bulk of the yellow quartz sand overlying the Tamala Limestone within the Spearwood Dunes has not been formally recognized as a separate formation, except in local areas such as Rockingham (Cooloongup Sand; Passmore 1970) and Australind (Eaton Sand; Semeniuk 1983). Lithologically similar yellow sands (Prider 1948, Glassford 1980) which are located east of Perth on the eastern margin of the Pinjarra Plain and in the foothills of the Darling Scarp (Low & Lake 1970, Low *et al* 1970, Wilde & Low 1978, 1980) have been assigned to the Yoganup Formation (Low 1971). For the sake of simplicity the Yoganup Formation yellow sands in this complex geomorphic setting are excluded from the present study.

The age of the yellow sands is interpreted to be mainly middle Pleistocene (Playford *et al* 1975). It forms much of the land surface of the coastal plain to landward of the Holocene coastal dune belt and the Pleistocene limestone ridges. Where the yellow sand underlies the coastal limestones it may range to Pliocene in age (Logan *et al* 1970, Glassford 1980).

The terrain of yellow sand on the coastal plain is the western fringe of a vast, diachronous cover of sand dunes and sand sheets which extend westwards from the central Australian Desert (Killigrew & Glassford 1976, Glassford 1980, 1987, Beard 1984). Thus yellow sand occurs extensively on the Yilgarn Block and forms an extensive and thick lithosnme that underlies and overlies coastal limestones and underlies landward parts of the coastal plain (Semeniuk & Glassford 1988).

On the coastal plain near the present coast, there is a shore-parallel belt of Pleistocene coastal limestone ridges (Tamala Limestone). These ridges, with variable cover of yellow sand, form shore outcrops, or may be buried by Holocene littoral and coastal-dune deposits. In cross section the coastal limestone complex forms a large lens mainly on, but also within, the western margin of the aeolian sand sheet described above, a relationship that is evident for much of the west coastal region of Western Australia from Shark Bay to Perth, a distance nf over 1 200 km (Logan *et al* 1970, McWhae *in* Quilty 1974, Glassford 1980, Allen 1981, Semeniuk & Glassford 1988). The eastern contact of the limestone-ridge-belt with yellow quartz sand nf the hinterland is complicated: *ie* it may be sharp, or lithologically gradational, marked by east-west interfingering, or marked by zones of scattered limestone lenses in yellow sand (Semeniuk & Glassford 1988).

The lithofacies referred tn herein as yellow sand, although typically yellow, also includes sands varying from red to brown to locally white. Grain sizes range from bimodal to poorly unimodal to unimodal, and the sand is typically fine skewed, well to poorly sorted and medium sized. Framework grains are predominantly quartz, with moderate to minor microcline and minor heavy minerals. The grains have a coating of silt-clay sized kaolin, goethite (yellow) and/or haematite (red) and quartz. These latter minerals also occur in the less than 0.09mm fraction of the sediment (Glassford 1980).

Description and interpretation of stratification in yellow sand

Contour data from 1:25 000 topographic sheets and field observations of surface morphology indicate that sites 1, 2, 3, 4 and 7 of this study are within large scale sand-sheet ramparts which drape the landward side of the coastal-limestone-ridge belt; sites 5 & 6 are in sinuous and parabolic landforms; and sites 8 to 15 are within an east- west oriented linear draa with stellate landforms (Table 1; Fig. 1). The term *draa* refers to large scale dunes or megadunes and compound or complex types of compnsite dunes (Wilson 1972, Leeder 1982, Lancaster 1988).

On the basis of presence/absence and inclination of large scale (>1m thick) sets of stratification, yellow sand is divisible into:

1) units with inclined strata ie cross-strata (high and low angled);
2) units with horizontal strata; and
3) units with massive structure.

These features are described below. Small scale (<0.3m thick) sets of cross-strata were not observed at any of the sites. The thinnest recognizable strata or laminae that comprise sets of cross-strata and horizontal strata in yellow sand are mostly evident due to differences in size of framework sand grains and, to a lesser extent, to varying amounts of yellow to brown silt-clay sized matrix fill of kaolin and goethite and variations in framework-grain coatings of kaolin and goethite.

Inclined strata

Description

Large scale sets of inclined strata (commonly referred to as cross-strata) occur extensively in 13 nf the quarries (Table 1). Sets of cross-strata typically are up to 5-10m thick, and generally, only occur at depths of more than 3-5m below the present landsurface. Cross-stratification consists dominantly of tabular-shaped sets of planar cross-strata with local minor occurrences of wedge-shaped and hummocky-shaped sets of planar and curved cross-strata (Figs 2, 3 & 4). Tabular-shaped sets of planar cross-strata have been traced continuously along recently exposed quarry faces for distances of 10 to 100 m. Generally exposures of cross-stratification are limited by an upper zone of bioturbatinn, or by lateral slumps of quarry walls, or by quarry floors.

Table 1

Sand quarries near Perth with large scale cross-stratification and major disconformities.

Quarries examined and their site numbers[1]	Large scale cross-stratification[2]	Major disconformities[3]
1 Wangara North	present	2 present
2 Wangara	present	3 present
3 Landsdale West	-	2 present
4 Landsdale East	-	1 present
5 Belhus	present	-
6 Henley Brook	present	1 present
7 Mirrabooka	present	5 present
8 Jandakot West	present	-
9 Jandakot East	present	-
10 Jandakot North 1	present	-
11 Jandakot North 2	present	
12 Canning Vale	present	1 present
13 Banjup West	present	1 present
14 Banjup East 1	present	1 present
15 Banjup East 2	present	1 present

[1] See Fig. 1 for location of sites.
[2] Large-scale is defined as greater than 1.0m thick.
[3] Number of major disconformities in the yellow sand sequences.

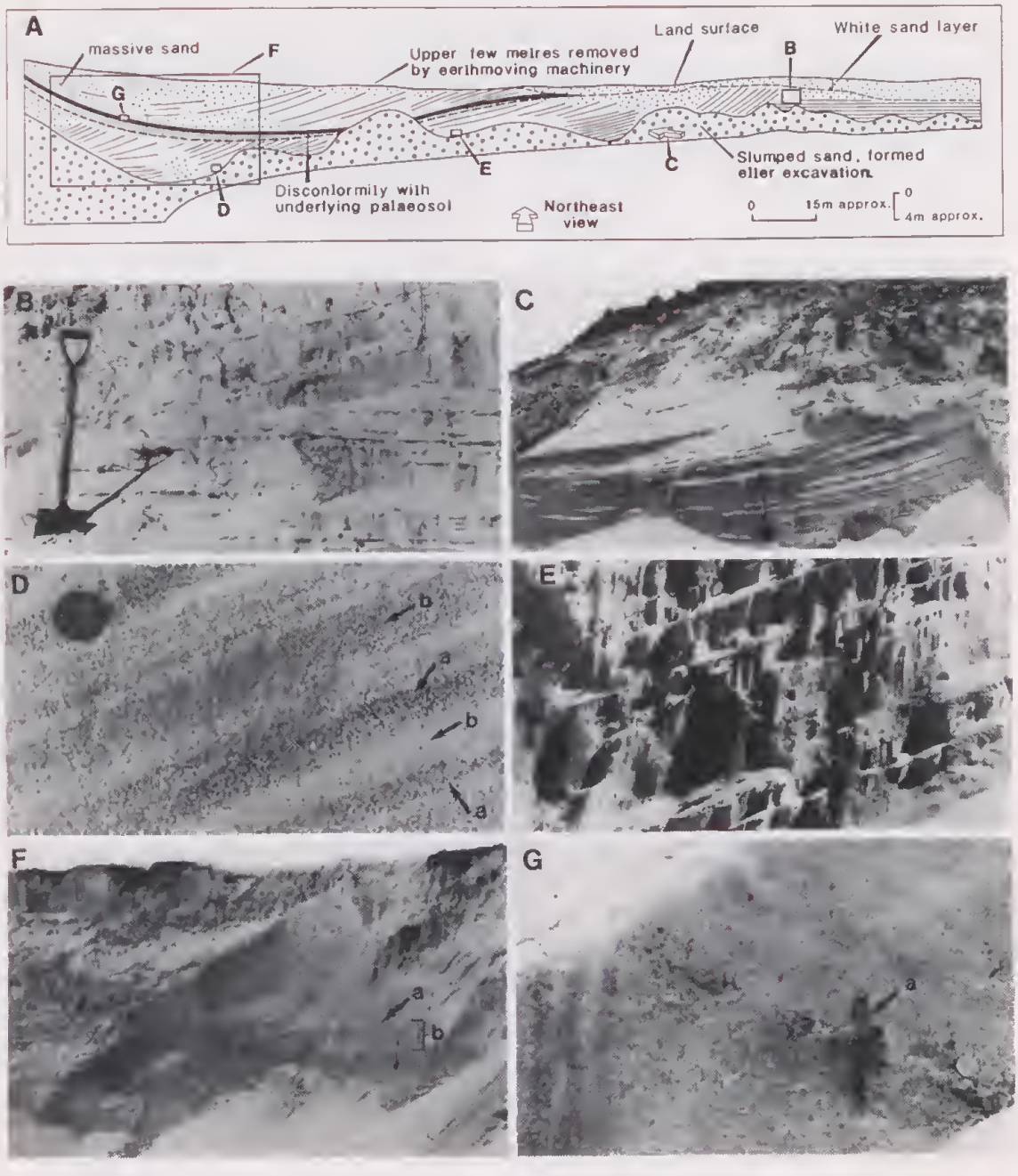

Figure 2 Range of stratification features at a single typical locality, Banjup West. See Fig. 1 for location. **A** Panoramic diagram of stratification and location of insets. **B** A large scale, tabular set of planar horizontal strata overlain by a large scale, wedge-shaped set of planar cross-strata (inclined strata). **C** A large scale set of concave-upwards, trough cross-strata. Note the rivulets of flowing sand which are building avalanche cones of sand. The continued growth of avalanche cones of sand will eventually conceal the stratification. **D** Thinnest recognizable strata in a large-scale set of low angle, planar cross-strata produced by differences in grain size of framework sand grains. The coarser layers (a) resemble ripple-form strata of Hunter (1977). The finer layers (b) resemble grainfall strata of Hunter (1977). Coin is 21mm in diameter. **E** Layering in a large-scale set of planar cross-strata produced by differences in texture, composition and colour. Thin prominent layers have framework quartz-sand grains supported in a silt-clay matrix of yellowish brown goethite, kaolin and quartz. Thick layers lack the silt-clay matrix. Coin is 28mm in diameter. **F** Disconformity (a) between two units of yellow sand. The discontinuity between the units is produced by: geometry of interface; changes in stratification details away from the contact; and structural, textural, compositional and colour differences between the two units on either side of the interface. The massive zone below the disconformity is a palaeosol (b) which indicates the disconformity is a regional bounding surface (Talbot 1985). Note also the common indistinct appearance of stratification. Several metres of surficial sand has been removed from this section by excavating machinery. Spade for scale is 1 m in length. **G** Closer view of disconformity surface, sloping from upper left to lower right and with underlying, mostly massive palaeosol with rare organic material and burrow-structures (a). Note rivulets of flowing sand on the left hand side. Coin is 24 mm in diameter.

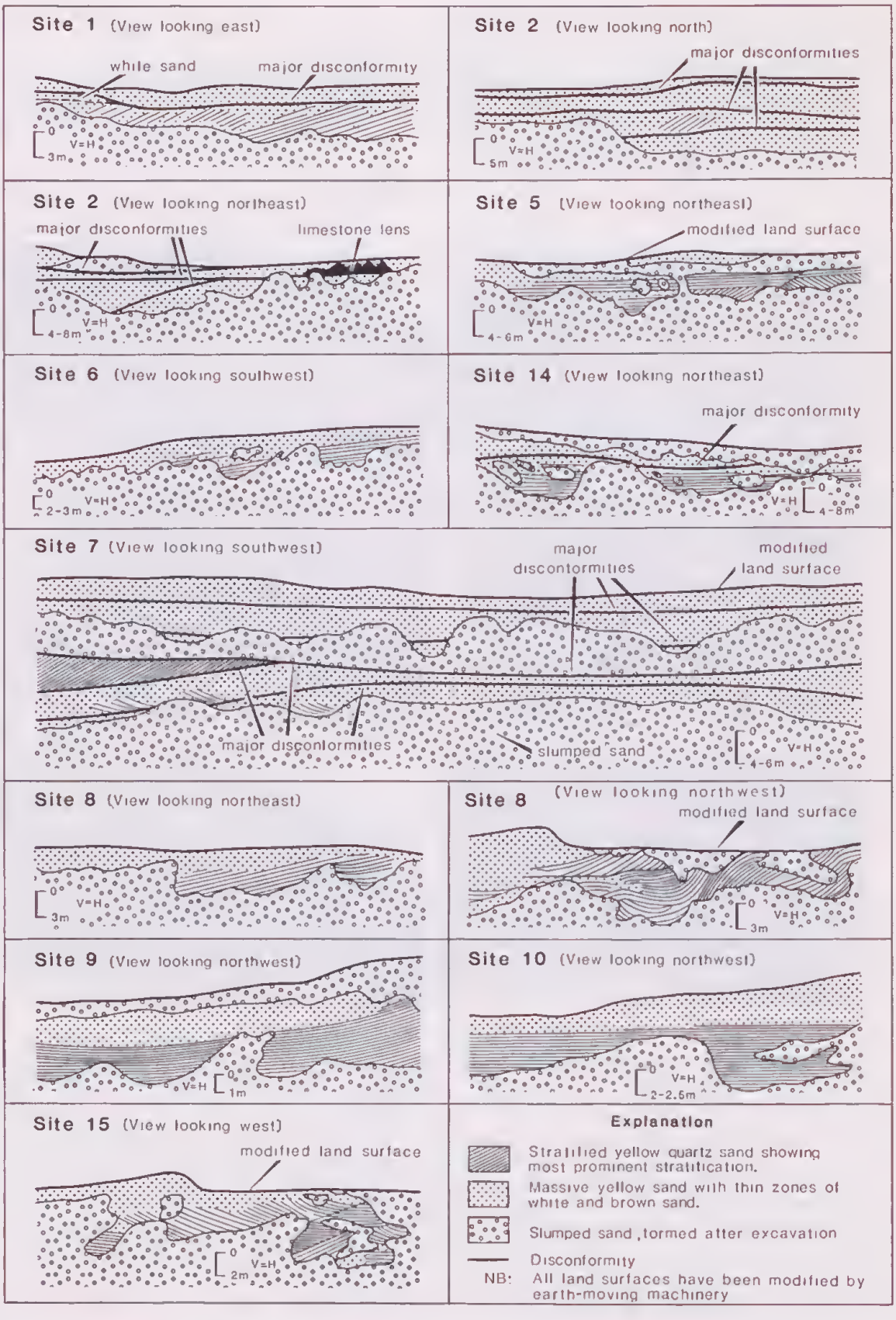

Figure 3 Panoramic diagrams of stratification attitudes and relationships within sequences of yellow sand, Swan Coastal Plain, southwestern Australia. See Fig. 1 for locations.

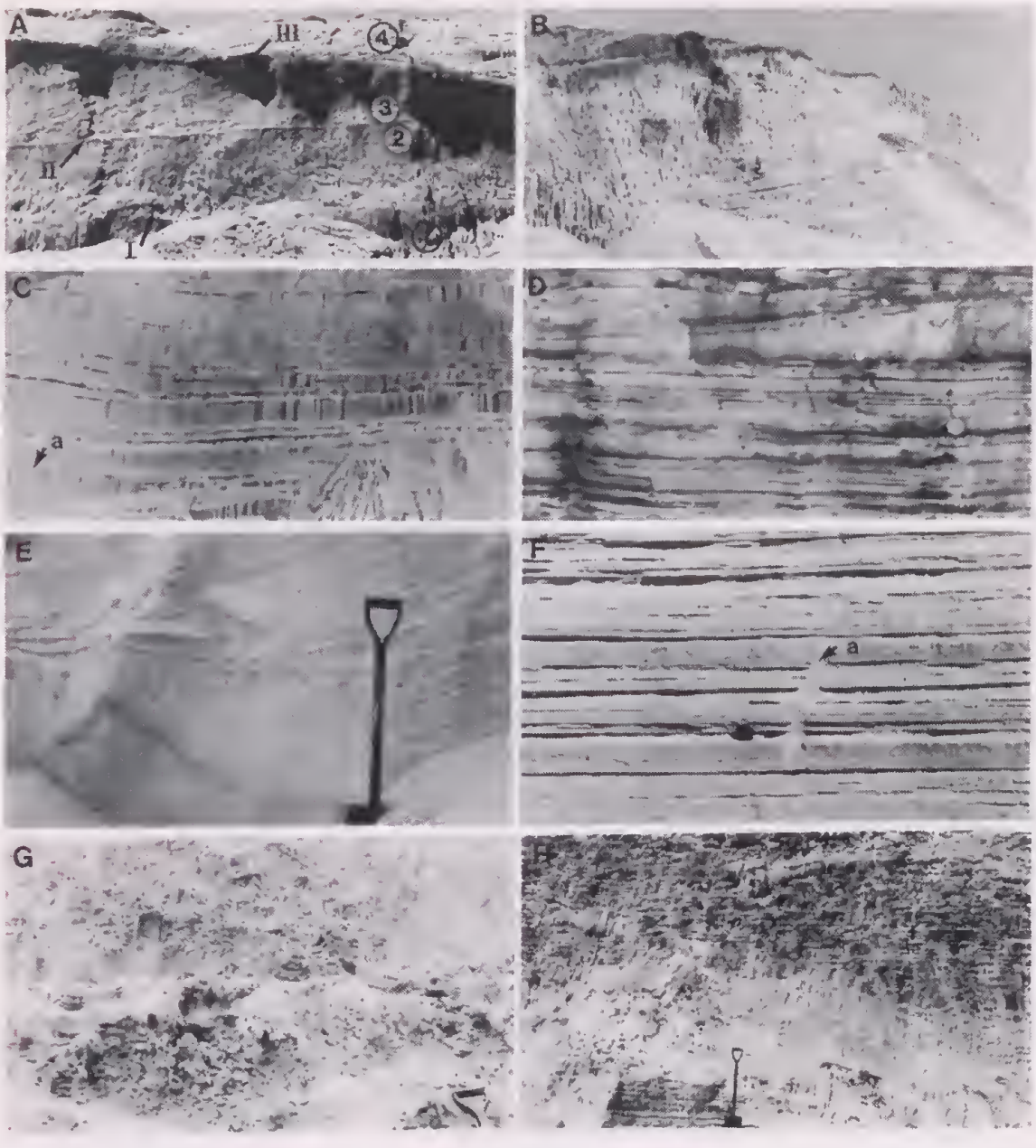

Figure 4 Primary stratification and secondary overprint fetures in yellow sand. See Fig. 1 for locations. **A** Four units (1, 2, 3, 4 of yellow sand bounded by three disconformities (I, II, III), Mirrabooka quarry. Note the common indistinct nature of the stratification. Unit 1 is mostly massive. Unit 3 has large scale, high angle planar and tangental cross-strata which dip towards the west (towards RHS). Unit 3 has large scale, high and low angle planar cross-strata which dip towards the east (towards LHS). Unit 4 has been truncated by earth-moving machinery. Spade for scale is 1 m in length. See Table 2 & Fig. 7. **B** Set of large scale, low angle, planar cross-strata dipping towards the southwest (towards LHS), Jandakot North 2. Note firstly, cross-stratification at depth is obscured by cone- shaped slumps of sand along the base of the cross-stratified sand escarpment. Secondly presence of an overlying soil of white and black sand which has been disrupted and partly removed by earthmoving machinery. Set is 7-8 m thick. **C** Set of large scale, broadly concave-upwards, trough cross-strata, Jandakot West. Note 28 mm diameter coin in lower left hand corner, below a broad trough-shaped bounding surface (a). Stratification is obscured by slumped sand on the lower right hand side. **D** Large-scale set of low angle and horizontal strata which resemble grainfall and plane bed strata of Hunter (1977). Strata underlie an interdune area, Canning Vale. Coin 28mm in diameter. **E** Rare cut-and-fill structure, Banjup West. Lower set of horizontal strata has been truncated by erosion (? surface wash) and then overlain by an upper westward dipping set of large-scale high angle, tangental to planar cross-strata. **F** Burrow structure (a) in horizontally stratified sand which has negligible goethite and kaolin silt-clay, Jandakot North. Layers resemble grainfall and plane bed strata of Hunter (1977). Coin is 28mm in diameter. **G** Termitarium structured yellow sand, upper few metres of unit 4, Mirrabooka. In contrast to F above the sand is relatively rich in goethite and kaolin silt-clay (see Table 2). **H** Large-scale set of low angle, planar cross-strata (lower one third) overlain by a large-scale set of horizontal strata (upper two thirds) which underlie an interdune and are partly ferruginized to form brown sandstone (*coffee rock*).

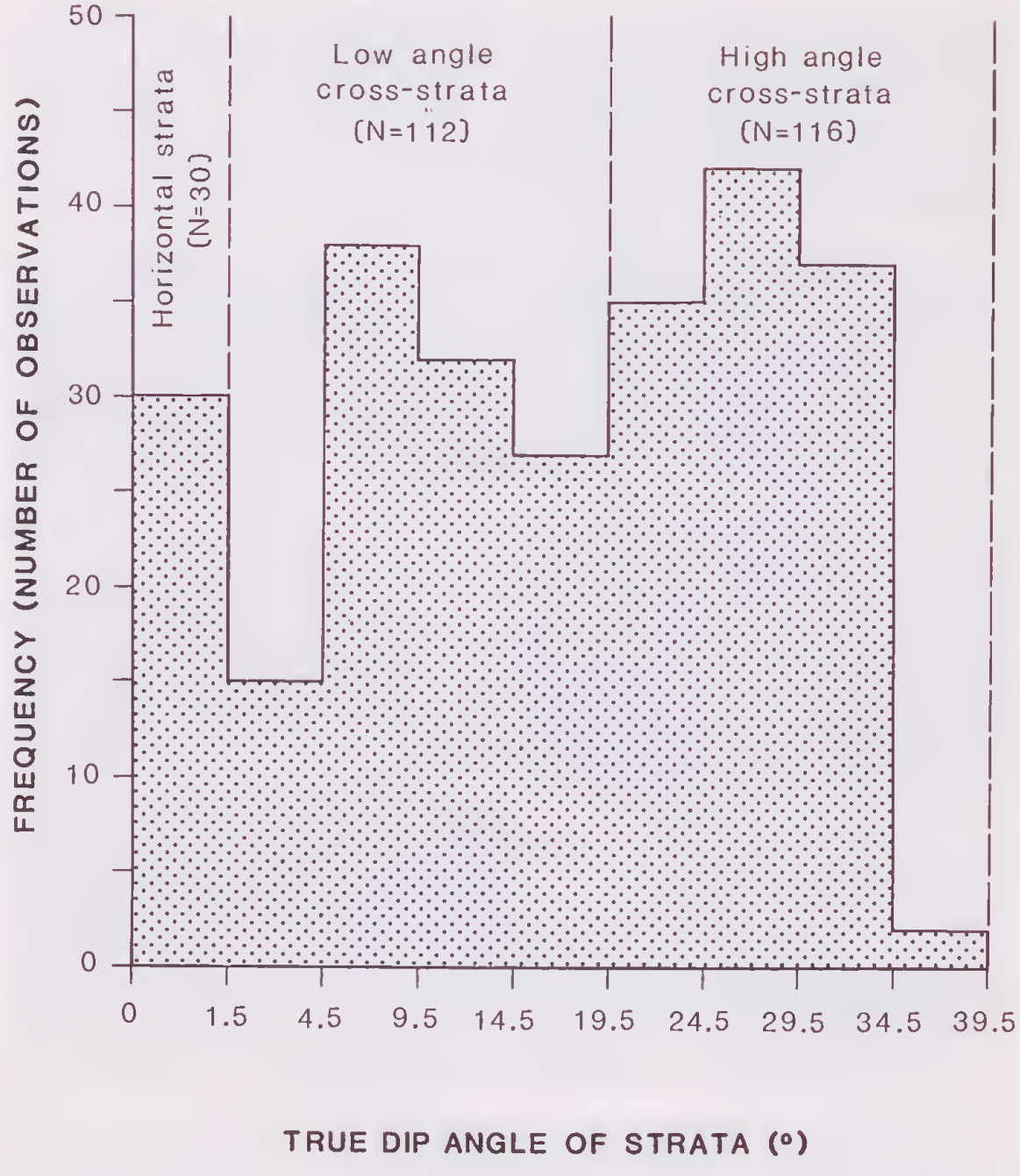

Figure 5 Frequency distribution of true dip angles for high angle (equal or greater than 20°) and low angle (1.6-19°) cross-strata and horizontal strata (0-1.5°) from yellow sands of the Perth area, Swan Coastal Plain, southwestern Australia.

Dip angles of cross-strata have a bimodal frequency. High angle (equal to or greater than 20°) cross-strata comprise *c* 51% of measurements and form a mode between 25-30° (Fig. 5). The highest dip angle recorded for cross-strata in yellow sand is 35°. Low angle (1.6-19°) cross-strata comprise 49% of measurements and form a mode between 5-10°, and the mode is skewed towards 10-15° (Fig. 5). The proportion of high angle strata is probably lower than these figures indicate because of a bias in the location of quarries towards hill tops rather than plinths and interdune flats.

The frequency of occurrence of dip directions (azimuths) of cross-strata at individual sites may be unimodal, bimodal or polymodal (Fig. 6). Individual disconformity-bounded sets of cross-strata at the same locality may have variable dip directions (Table 2; Fig. 7). At six sites cross-strata have mean resultant dip direction towards the W and SW. At three sites cross-strata have mean resultant direction towards the E and SE. At two sites cross-strata have mean resultant dip direction towards the NE. At one site the resultant dip direction changes between the various disconformity bounded units of yellow sand (Fig. 6). Dip

Table 2

Description of lithology for the sequence of yellow sands at Mirrabooka quarry. See Fig. 1 for location. Grain size terminology after Folk (1974).

DEPTH (m)	DESCRIPTION	LITHOFACIES
0 to 4.0*	Quartz sand; yellow, massive, sand-framework supported, unimodal, near symmetrical to fine skewed (range +0.0 to +0.12), well sorted to moderately well-sorted (range 0.47 to 0.61 phi), medium (range 1.21 to 1.63 phi) quartz sand with 0.9% fines** (range 0.60 to 1.18%); framework quartz-sand grains of yellow sand have a surface coating of goethite (yellow) pigmented kaolin plus silt-clay sized quartz	Unit 6
	DISCONFORMITY (V)***	
4 to 9	Quartz sand; white in upper 0 to 0.3m then yellow to 9m, massive, sand-framework supported, unimodal, near symmetrical (range +0.02 to -0.05), moderately well-sorted (range 0.58 phi to 0.60 phi), medium (range 1.56 to 1.63 phi) quartz sand with 1.18% fines (range 0.97 to 1.35%); framework quartz-sand grains of yellow sand have a surface coating of goethite (yellow) pigmented kaolin plus silt-clay sized quartz; the white sand does not have a yellow coating on grains.	Unit 5
	DISCONFORMITY (IV)	
9 to 14	Quartz sand; in places upper 0 to 0.3m white then yellow and yellowish red with white mottles to 14m; in places upper 0 to 0.5-1.0m is termitarium structured with a tortuous network of vermiform voids or loose sand fill and labyrinthoid walls of coherent sand and silt-clayey sand; from 9.10 to 12.5m conspicuously cross stratified with large scale high angle strata dipping towards the southeast; from 12.5 to 14m conspicuously cross-stratified with large scale low angle strata dipping towards the southwest; sand-framework supported, unimodal to poorly unimodal, fine skewed to near symmetrical (range +0.15 to -0.05), moderately well-sorted to moderately sorted (range 0.54 to 0.72 phi), medium (1.33 to 1.66 phi) quartz sand with 1.55% fines (range 0.88 to 2.08%); in places thin beds of coarse sand, framework quartz sand grains of yellow to red sand have a surface coating of goethite, haematite, kaolin and silt-clay sized quartz; white sand does not have coating on grain surfaces.	Unit 4
	DISCONFORMITY (III)	
14 to 17.5	Quartz sand, brownish yellow to reddish yellow to brown with white mottles; conspicuously cross-stratified, from 14 to 17.5m large scale, high and low angle strata dip towards the northeast and east, in places from 16 to 17.5m large scale, low angle cross-strata dip towards SSE; sand framework supported, unimodal, near symmetrical (range +0.03 to +0.06), moderately well-sorted (range 0.52 to 0.60 phi), fine to medium (range 1.69 to 2.03 phi) quartz sand with 2.24% fines (range 1.84 to 2.74%); framework quartz-sand grains of yellow to brown sand have a surface coating of goethite and kaolin plus silt-clay sized quartz; white sand mottles have grains which do not have surface coatings	Unit 3
	DISCONFORMITY (II)	
17.5 to 20.5	Quartz sand; pale yellow to reddish yellow; generally massive, in places faintly cross-stratified with high angle strata dipping towards the W & WNW; sand-framework supported, unimodal, near symmetrical to strongly fine-skewed (range +0.08 to +0.61), moderately well-sorted (range 0.64 to 0.69 phi), medium (range 1.41 to 1.7 phi) quartz sand with 2.85% fines (range 2.53 to 3.13%); framework quartz sand grains of yellow sand have a surface coating of goethite, haematite, kaolin and silt-clay sized quartz	Unit 2
	DISCONFORMITY (I)	
20.5 to 26+	Quartz sand; yellow to red, white in the vicinity of the ground water table (c 24.2cm); generally massive, in places faintly cross stratified with large scale, high angle strata dipping towards the NW, sand framework supported, unimodal to poorly unimodal, near symmetrical to strongly fine skewed (range +0.06 to 0.37), moderately well sorted to moderately sorted (range 0.61 to 0.97 phi), coarse to medium (range 0.97 to 1.36 phi) quartz sand with 3.15% fines (range 1.12 to 6.57%); framework quartz-sand grains of yellow to red sand have a surface coating of goethite (yellow) or haematite (red) pigmented kaolin plus silt-clay sized quartz, white sand in vicinity of groundwater table has grains which do not have a surface coating; groundwater table c 0.5m below base of quarry.	Unit 1

* Natural surface has been removed

** Fines equal weight percentage of grain size less than 0.09mm. Generally fines of yellow to red sand are composed of c 50% kaolin, goethite and/or haematite and c 50% quartz and heavy minerals. Fines of white sand are composed of quartz and heavy minerals. Note that there is a uniformly consistent decrease in the amount of fines from unit 1 at depth to unit 6 near the surface. Furthermore modern beach-berm sands average 0.09% fines (range 0-0.48%) and Holocene coastal dunes average 0.15% fines (range 0-0.62%), see details in Glassford (1980)

*** Discontormities recognised by occurrence of palaeosols, undulating discontinuity surfaces, changes in structure (eg massive to cross-stratified) and changes in fabric, texture, composition and colour.

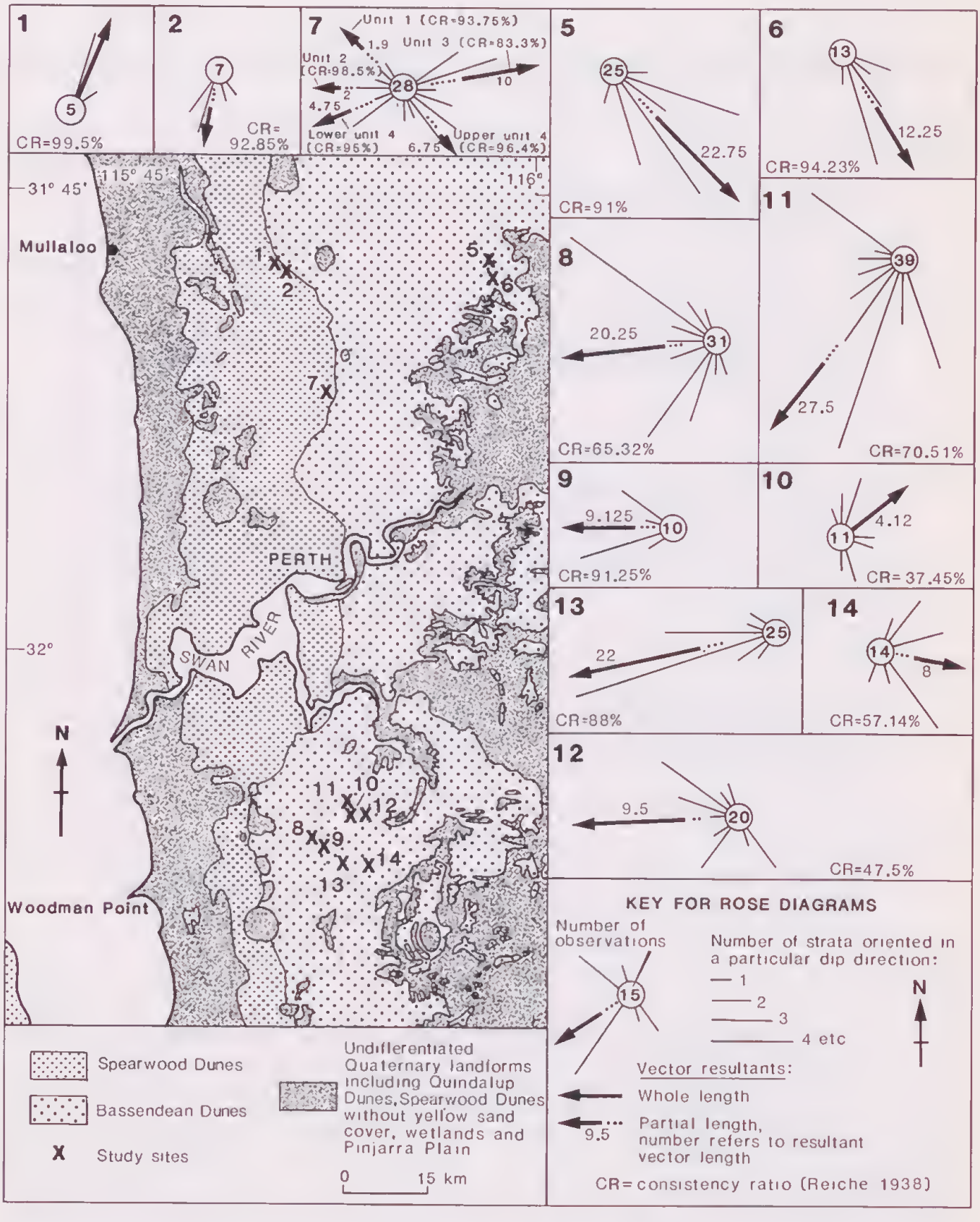

Figure 6 Rose diagrams of dip directions of cross-strata for individual sites in the Perth area, Swan Coastal Plain, southwestern Australia. See Fig. 1 for locations. Map boundaries are after Wilde and Low (1978, 1980).

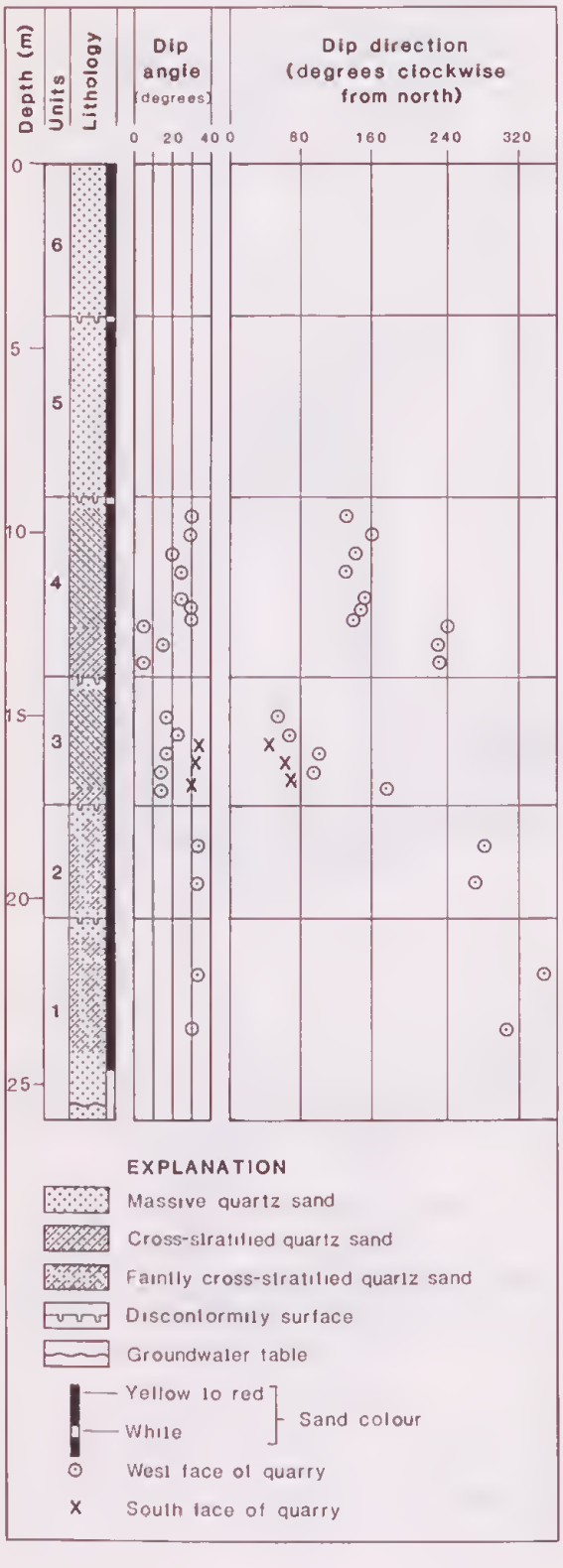

Figure 7 Vertical section of six disconformity-bounded units of yellow sand and the dip angles and dip directions of cross-strata for the respective lithostratigraphic units of yellow sand. Note that the yellow sands are massive near the surface stratified at depth and then massive near the groundwater table.

directions may vary markedly between and within units of yellow sand at the one site. For instance at Mirrabooka (Fig. 1) the lower strata of unit 4 dip towards 240° whereas middle to upper strata dip towards 160° (Table 2; Figs 6 & 7).

The dip directions of all cross-strata have a polymodal frequency distribution. High angle and low angle cross-strata also have a polymodal frequency distribution (Fig. 8). High angle cross-strata have prominant modes between 135° and 171°, between 243° and 261°, skewed to 279° and between 297° and 315°, skewed to 279° (Fig 8A). Low angle cross-strata have prominant modes between 135° and 153°, skewed to 171°, between 189° and 207°, skewed to 225° and between 297° and 315° (Fig. 8B).

The mean vector resultant is (Figs 8 & 9):

- towards 220° for high angle, large scale cross-strata
- towards 198° for low angle, large scale cross-strata and
- towards 210° for all large scale cross-strata.

Interpretation

High angle, large scale cross-strata are interpreted to be the lee-slope foresets of aeolian dunes (following McKee & Bigarella 1979, Nielson & Kocurek 1987). Dip directions of the high angle cross-strata indicate deposition by SE winds, ENE winds and NNW winds (Table 3). Low angle cross-strata are interpreted to be predominantly a combination of lee-slope foresets, dune (including star dune) foot-slope plinths and sand-sheet sets (following Ahlbrandt & Fryberger 1981, Kocurek 1981, Nielson & Kocurek 1987). Dip directions are roughly similar to those of high angle cross-strata and indicate deposition by SE winds, NNE winds, and NW winds (Table 4). Mean vector resultants for high angle, low angle, and high angle plus low angle cross-strata indicate long-term overall sand movement, on average, was from NE towards SW (Table 5; Figs 8 & 9). This is opposite to the direction of transport of carbonate sands of the present modern coastal dunes, which is towards the NE (Searle & Semeniuk 1985).

Table 3

Formative wind directions and predominant direction of sand movement for large scale high angle cross-strata.

Modal dip directions of large scale high angle cross-strata[1]	Formative wind direction	Direction of sand movement
Towards 306° (towards NW)	From SE	From SE to NW
Towards 252° (towards WSW)	From ENE	From ENE to WSW
Towards 162°-144° (towards SSE)	From NNW	From NNW to SSE

[1] Modes are from Fig. 8

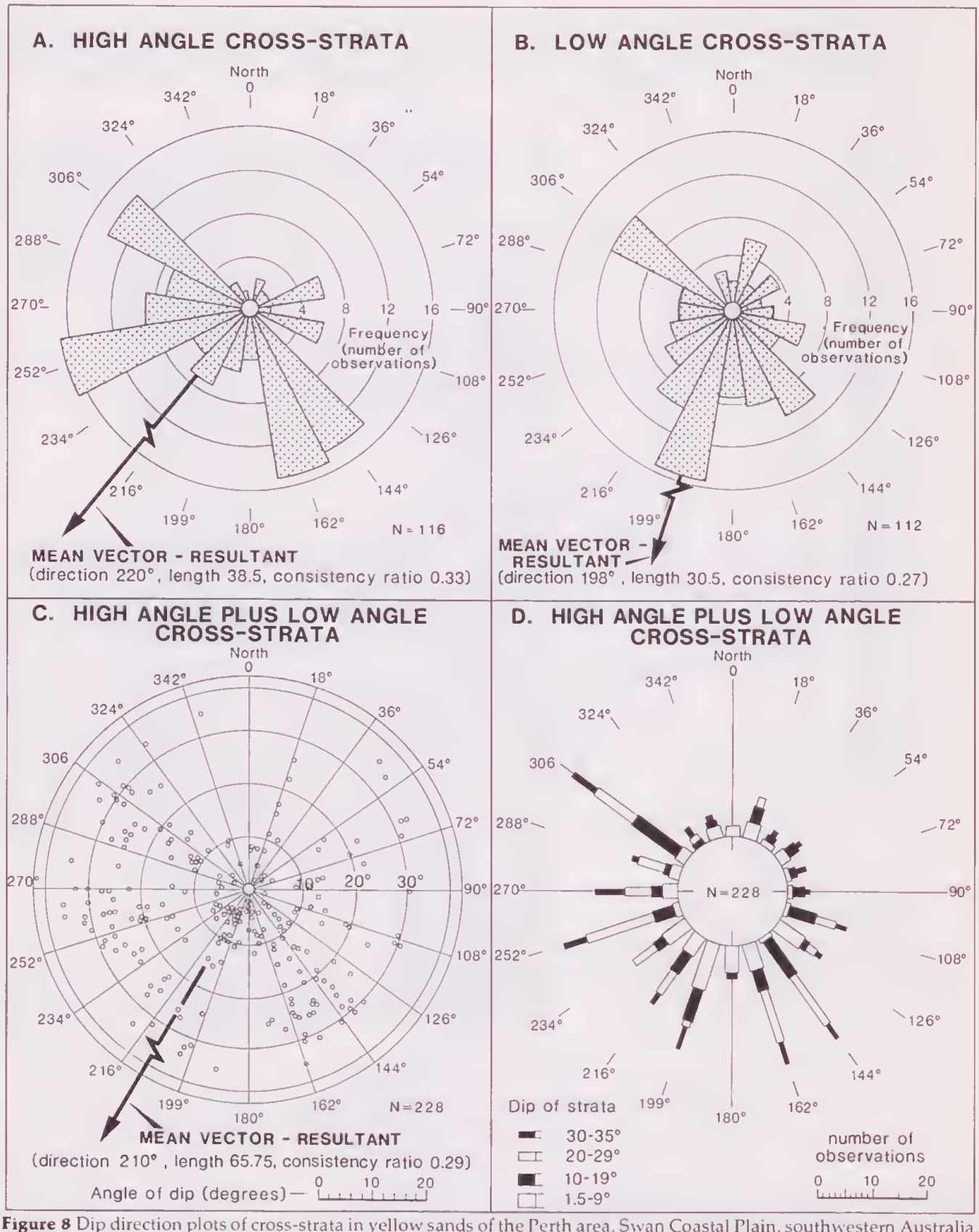

Figure 8 Dip direction plots of cross-strata in yellow sands of the Perth area, Swan Coastal Plain, southwestern Australia. A Rose diagram of dip directions of high angle (equal to or greater than 20°) cross-strata. B Rose diagram of dip directions of low angle (1.6-19°) cross-strata. C Scatter plot diagram of dip angles and dip directions for all cross-strata. D Rose diagram of dip angles and dip directions for all cross-strata. Note A & B are plotted with an arithmetic scale, and not an equal-area scale (*cf* Nemec 1988).

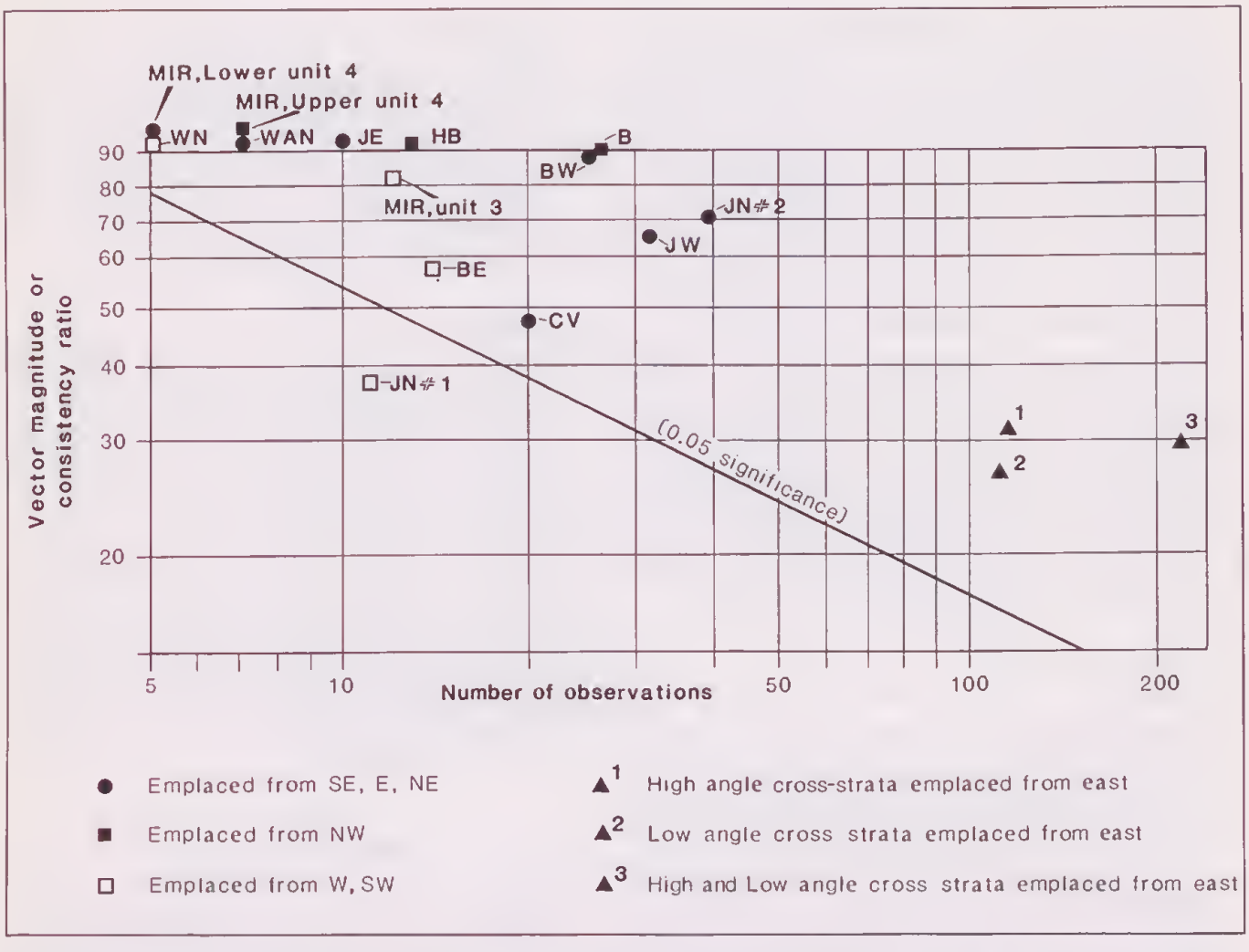

Figure 9 Graph of vector magnitude (consistency ratio of Reiche 1938) versus number of observations of dip direction to show significance (at 0.05) of the vector magnitude (following Lindholm 1987). Note the vector magnitudes which plot above the 0.05 probability line, indicate there is less than 1 chance in 100 that the population does not have a preferred direction of movement.

Table 4

Formative wind directions and predominant direction of sand movement for large scale low angle cross-strata.

Modal dip directions of large scale low angle cross-strata[1]	Formative wind direction	Direction of sand movement
Towards 306° (towards NW)	From SE	From SE to NW
Towards 216°-199° (towards SSW)	From NNE	From NNE to SSW
Towards 144° (towards SE)	From NW	From NW to SE

[1] Modes are from Fig. 8

Table 5

Directions of mean vector resultants for high angle, low angle, and high angle plus low angle cross-strata and their palaeo-directional interpretations.

Cross-strata	Direction of mean vector resultant[1]	Interpretation
High angle	Towards 220° (towards SW)	Overall sand movement is from NE to SW under the influence of Pleistocene winds which were predominantly from the eastern sector
Low angle	Towards 198° (towards SSW)	Overall sand movement is from NNE to SSW under the influence of Pleistocene winds which were predominantly from the eastern sector
High angle plus low angle	Towards 210° (towards SSW)	Overall sand movement is from NNE to SSW under the influence of Pleistocene winds which were predominantly from the eastern sector

[1] Vector resultants are from Fig. 8.

The overall sand movement from NE has many local variations (Figs 6 & 7). Sites which are closely located (*eg* 10, 11, 12, 13 & 14; Fig. 6) may have a wide divergence in direction of their dip direction resultants. Furthermore the dip directions of individual sites (*eg* sites 8-14; Fig. 6) are also widely divergent, typically over more than 180° . Interconnected (by one or more arms) stellate dune morphology, plus the associated wide range in dip directions of the internal strata of the same features, suggests that sites 8-14 are located within a linear draa (or megadune) with star dunes. This interpretation is important, because the internal structures of star dunes are imperfectly known and only rarely have they been identified in the sedimentary record (Nielson & Kocurek 1987).

It has been previously suggested elsewhere that yellow sand is predominantly glacial age desert-aeolian sediment (Glassford & Killigrew 1976, Killigrew & Glassford 1976, Glassford 1980, Semeniuk & Glassford 1988). Cross-strata details (Figs 6, 7, 8 & 9) provide additional support for a desert-aeolian origin and are consistent with the following refinements to the desert aeolian model in terms of more specific formative wind directions. During periods of deposition of yellow sands, Pleistocene wind directions were dominantly from the eastern sector, sub-dominantly from the NW and to a minor extent from the W and SW.

Horizontal strata

Description

Horizontal strata (*c* 0-1.5° angle of dip) comprise *c* 13% of all strata measured (Fig. 5). As discussed later this low proportionate amount is probably an artifact of the location of quarries in hills of sand rather than sand flats. Sets of horizontal strata are up to 7 m thick, and have been traced laterally for up to 50 m and, by interpolating discontinuous outcrop, for more than 100 m (Figs 2 & 3). Horizontal strata mainly consist of thin to very thin beds and laminae (Figs 4C, D & E). Individual strata typically are planar. Sets of horizontal strata may be separated by low angle stratification (Fig. 4C) and they usually grade laterally into concave-upward low angle strata (Site 9 of Fig. 3).

Interpretation

Large scale sets of horizontal strata are interpreted to be dune bottom-set deposits and interdune, aeolian sand-sheet deposits formed mainly by grainfall and the movement of wind ripples, plane beds/laminae and dunes across the surface of interdune sand sheets (following Glennie 1970, Hunter 1977, Ahlbrandt & Fryberger 1981, Kocurek 1986, Lancaster 1988). The movement of sand as ripples and plane beds or laminae across sand sheets produces horizontal strata during moderate to strong wind action (Bagnold 1941, Glennie 1970, Jopling 1978). In terms of this study, the direction of sand transport cannot be inferred from horizontal stratification.

Sand flat terrain, if geomorphically analogous to the sand flats of some desert areas (*eg* McKee & Tibbits 1964, Ahlbrandt & Fryberger 1981), can be expected to be underlain predominantly by horizontal strata, and these strata would pass laterally into dune terrains underlain by cross-strata. That is, cross-stratified dunes typically grade laterally into horizontally stratified sand sheets of interdune areas (Figs 2 & 3). Quarries located in sand hills may be expected to have few horizontal strata. In desert ergs cross-stratified dunes and plinths may pass laterally into horizonatally stratified interdunes, and both may be underlain by horizontally stratified sheets of sand.

Massive structure

Description

Sand units with massive structure have no internal stratification. These units occur in three main settings: below the present landsurface to a depth of 3-5 m; as thin sheets typically 0.5-2 m thick beneath buried unconformity surfaces; and up to several metres above the water table (Table 2, Fig. 7). Sequences of sand below the water table have not been observed *in situ*. Units with massive structure commonly exhibit a range of bioturbation features, as will be discussed later.

Interpretation

The massive structure of yellow sand is an overprint feature and predominantly the product of bioturbation. Thus massive yellow sand may have originally been stratified. This interpretation is consistent with the yellow sand dunes and sheets being relict, and with the common association of bioturbation overprints with relict desert aeolian deposits (Glennie 1970, Fryberger *et al* 1979, Glassford 1980, 1987; Ward 1988). Buried units of massive yellow sand, which are overlain by stratified yellow sand, indicate an alternating history of desert aeolian deposition followed by bioturbation during subsequent intervening periods of semi-arid or humid conditions. The stratigraphic sequence of structures thereby also is consistent with the concept of alternations from glacial age desert phases to interglacial age humid phases. Such alternations characterise the late Cainozoic of many low and middle latitude areas of the world (Lamb 1977, Sarnthein 1978, Glassford 1980, Thomas & Goudie 1984).

Major disconformities

Description

Major disconformities occur in 13 quarries (Tables 1 & 2; Fig. 7). These disconformities may be within several metres of the present landsurface (Figs 2, 3 & 4), but more commonly occur near or disappear below the floor of quarries. Disconformities have been traced continuously along quarry walls for distances of up to 100 m and by extrapolating discontinuous exposures for over 300 m (Figs 2 & 3). Their observable extent is always limited by the dimensions of the quarry. Deep sequences of yellow sands also have more disconformities than shallow sequences.

Disconformity surfaces are broadly undulose with straight planar segments grading to curved segments (Figs 2, 3 & 4). Straight planar segments may be near-horizontal or inclined at angles of up to 15°. Curved segments are typically concave-up with maximum amplitudes of 5-6m over 50-60m. Disconformities typically have a discordant relationship with more than one set of cross-strata. Furthermore, they also typically separate units of yellow sand which are lithologically distinct in terms of structure (*eg* cross-stratified or massive), textures (*eg* coarser or finer, clay-rich or clay poor), composition and colour (*eg* reddish haematite-pigmented or yellow goethite-pigmented kaolin as coatings on framework grains and as fine sand to silt-clay sized grains). Disconformity surfaces within sequences of yellow sands are commonly underlain by a thin, discontinuous sheet of massive white quartz sand which typically is several centimetres to a few decimetres thick. In places the lower boundary of such sheets has decimetre to metre deep pockets and pipes of white sand, 5-20 cm in diameter, which taper downwards into underlying yellow sands.

Interpretation

Disconformities are marked by palaeosols (identified from overprint features; Table 6). They are buried former land surfaces, similar to the present vegetated land surface below which there are pedogenic overprints. These disconformities are super-bounding surfaces (Kocurek 1988), and most are similar to the regional bounding surface (Talbot 1985) category of super-surfaces. Disconformity surfaces have formed by erosion and soil development during interstadial or interglacial intervals under semi-arid or wet conditions similar to the present. Disconformities which are not underlain by a palaeosol, but are erosional, may represent one or more glacial or interglacial intervals. These disconformities are similar to the first order bounding surfaces of Brookfield (1977), and the first and second order bounding surfaces of Kocurek (1981).

Table 6

Description and interpretation of secondary alteration features, on or within yellow sand, which have overprinted primary stratification.

Overprint feature	Burrow structure
Description	Occurs up to 3-6m below the surface or below deeply buried surfaces (disconformities); burrow-like structures range from less than 1cm to several centimetres in diameter; depending on the plane of section burrows may be round to cylindrical; burrow-fill may differ from surrounding sand in terms of texture, colour and grain types; burrows have a sharp contact with surrounding sand.
Interpretation	Burrowing by various insects, spiders and vertebrates and infilling of burrows when repeated destroys cross-strata and produces a pervasive burrow-mottled structure in detail at the mesoscale, and a massive structure at the macroscale.
Overprint feature	Fibrous root structure (a variety of root structure)
Description	Occurs up to 3-6m below the landsurface or 3-6m below buried disconformities; thin 0.5-1cm diameter vertical to branching cord-like (dendritic) sand, more coherent than surrounding sand when subjected to subaerial exposure; dendritic sand may differ from surrounding yellow sand mainly by being white.
Interpretation	Growth of fibrous plant roots displaces cross-strata and following death and decomposition the root channels are infilled with sand resulting in a dendritic structure of slightly more coherent sand at a mesoscale; at a macroscale the sand appears massive.
Overprint feature	Tap root structure (a variety of root structure)
Description	Occurs to depths of more than 12m below the present landsurface; tap root structures typically are 5-20cm in diameter and this size extends continuously over vertical distances of more than 12m; the structures are typically tube-like with a white sand fill and ferruginous sand rim; the pipe-like structures typically have a vertically discordant relationship with horizontal strata
Interpretation	Growth by tap roots displaces strata; these tap roots act as conduits and sites for solutions and suspensions of iron and aluminium minerals thereby producing multiple vertically discordant pipes of white and ferruginous sand
Overprint feature	Colour mottles
Description	Occur firstly in a broad sheet-like zone up to 6-8m above the groundwater table; secondly in a broad sheet-like zone up to 3-8m below the landsurface or buried landsurfaces; mottles are typically variable in size and shape; mottle diameters range from a few mm to several decimetres, mottle shapes range from equant through pipe-like to highly indented amoeboidal; mottles are typically white quartz sand differing from surrounding yellow sand only in terms of colour and goethite, haematite and kaolin content
Interpretation	Vadose zone and the zone of capillary rise of intermittent wetting and drying and fluctuating Eh and pH in the phreatic zone results in differential pedogenic removal of silt-clay sized coatings of goethite, kaolin and quartz from the surface of sand grains.
Overprint feature	Massive structure
Description	Occurs up to 4-6m below the present landsurface and the surface of buried units of yellow sand, may grade vertically or laterally into units of root structured and/or burrow-structured yellow sand and/or colour mottled sand.
Interpretation	Physical perturbations (*eg* wetting and drying, removal of fines, settling, compaction) and biological perturbations (*eg* root-growth, burrowing) destroy cross-strata by disrupting and mixing sand layers to form a uniformly homogeneous yellow sand.
Overprint feature	Termitarium (or labyrinthoid) structure
Description	Occurs up to 2-4m below the present landsurface or below buried landsurfaces of yellow or brown sand/sandstone which are relatively rich in silt-clay sized goethite and/or kaolin; labyrinthoid structure comprises a tortuous pattern of vermiform channels to vesicular voids with brown or yellow sand/sandstone (*coffee rock*) walls and fill; typically weakly coherent; termitarium or labyrinthoid structure typically forms a 0.5 to 1.5m thick sheet roughly parallel to the present landsurface. The upper surface of this sheet typically is c 0.5-2m below the present landsurface.
Interpretation	Termites build a maze of channels with coherent walls, and over time destroy stratification; this results in a sheet of labyrinthoid structured sand/sandstone.

Overprint feature	Brown nodules and brown cementation to form sandstone (*coffee rock*)
Description	Occurs mainly in a sheet like zone between 0.5 to 2m thick and tends to be thicker in interdunes; brown to yellowish brown ferruginous quartz sand nodules supported in brown to yellow sand or brown ferruginous, massive, labyrinthoid quartz sandstone; nodules consist of quartz sand supported in a silt-clay matrix of goethite, kaolin and quartz; overlies yellow sand and underlies white sand; upper boundary may be smooth abruptly gradational and broadly parallel with the landsurface or interfingered with white sand over vertical distances of 1-2m, the lower boundary is abruptly gradational to yellow sand and roughly parallel to the upper boundary.
Interpretation	Silt-clay sized matrix material and framework grain coatings of goethite, kaolin and quartz have been removed from yellow sand and transferred in pore water solution and suspension and deposited, in the vadose zone mainly as sandy nodules to produce brown nodular sand, and in the phreatic zone to produce brown sandstone. Both types of overprint are types of *laterite duricrust* (locally termed *coffee rock*). These *laterite duricrusts* are altered desert-aeolian sediment because they consist of framework grains of desert-aeolian sand surrounded by remobilized and mineralogically partly transformed desert-aeolian dust. The overprints support the view of Playford *et al* (1975) that some *laterites* in South-western Australia are of Pleistocene age.
Overprint feature	White quartz sand
Description	White quartz sand is massive, and is without a grain-surface coating of goethite, kaolin and quartz of silt clay size. White quartz sand occurs in three settings, firstly, it is 1-2m thick where it occurs within a few metres of the landsurface; secondly, it is 0.5m thick where it marks buried former landsurfaces (at disconformities); thirdly, it occurs near the water table where it is c 1-4m thick. Near the present landsurface white sand thickens from dune tops to dune flanks to interdune flats, it also typically overlies brown nodular sand or brown sandstone and is overlain by humic sand; its upper boundary is smooth and broadly parallel to the landsurface, and gradational into humic sand; its lower boundary is sharp or abruptly gradational, and irregular or deeply (1-2m) penetrative in the form of 10-30cm diameter white-sand filled pipes into underlying brown sand. The upper boundary of white sand in the vicinity of the groundwater table may be sharp or broadly gradational into yellow sand
Interpretation	Yellow sand has been transformed to white sand by removal of grain coatings of goethite, kaolin and quartz silt-clay in pore water solution and suspension
Overprint feature	Humic quartz sand
Description	Massive and fibrous-root structured, grey to black quartz sand with plant debris and silt clay sized organic material; the quartz sand generally is not coated with goethite and kaolin. The unit forms a sheet-like cover 0.1 to 2m thick over white or yellow sand; it increases in thickness from Spearwood Dune ridges and Bassendean Dune tops into flanks and interdune and ridge flats; humic quartz sand overlies white or yellow quartz sand with a gradational contact, its upper boundary is the present landsurface, and its lower boundary is broadly parallel to landsurface
Interpretation	Yellow or white quartz sand has been impregnated by plant debris and silt-clay sized organic material to form a pedogenic A-horizon

The occurrence of up to six units of yellow sand separated by five major disconformities (Table 2, Fig. 7) is interpreted as the record of six major glacial-age desert aeolian phases and five major interglacial-age semi-arid or humid phases in yellow sands of the Perth region. These units are most likely only the upper portion of the record of desert-aeolian sedimentation in SW Australia (see Logan *et al* 1970, Glassford 1980, 1987).

Features which overprint sedimentary stratification

Sedimentary stratification in yellow sand grades into, and generally is gradually obliterated by pedogenic and other alteration (or overprint) features (Fig. 10). Overprint features include: burrow structures; root-structures; colour mottles; massive structure; termitarium structures; cementation by brown limonite and clays to form nodules and sandstone; removal of yellow or red grain coatings to form white quartz sand; and humic infiltration/addition to form humic quartz sand (Table 6). The obliteration is gradational. It decreases downwards below the present landsurface and beneath buried disconformies, and increases towards the groundwater table. Furthermore, thin, deeply buried disconformity-bounded units of sand lack internal stratification, but may be sharply overlain and gradationally underlain by stratified yellow sands. These relationships indicate that stratification is a primary feature and that it is overprinted by a variety of secondary features. Bioturbation is further described below.

Yellow sand from 3 to 5 m below the present land surface, and sands immediately below the buried surface of a disconformity, generally are massive to mottled to variously bioturbated. With increasing depth below the present land surface and below buried disconformities, the massive sand eventually grades into stratified sand. Quarry walls expose living tap roots, dead tap roots, sand-filled tap-root-like structures, and sand-filled to open insect burrows that penetrate the layered sands, with sediment-fills infiltrating from higher horizons. Gradational sequences, from laminated sand, through laminated sand with root and burrow structures to mottled sand and massive sand, indicate the progression of overprinting of stratification predominantly by bioturbation (Table 6; Fig. 10). Much of the yellow sand therefore records a history of disruption, mixing, and homogenizing by biological, chemical and physical processes which have overprinted and destroyed primary aeolian stratification.

Discussion and conclusions

The results of this study have many and far reaching implications. The pervasive occurrence of sedimentary stratification in thick sequences of yellow sands in the Bassendean and Spearwood dunes has implications for the origin of these sands. This is because the occurrence of stratification supports a primary aeolian origin, and precludes an origin wholly by *in situ* decalcification of limestones.

Dip direction resultants of the cross-strata of yellow sands indicate winds were dominantly from the eastern sector, sub-dominantly from the NW, and to a minor extent from the SW and W. This precludes a wholly coastal-marine derivation for yellow sand because the easterly component is opposite the SW to NE movement of carbonate sands of the modern coastal dunes (Searle & Semeniuk 1985). Presumably the movement of sands that formed Pleistocene coastal dunes (now limestone) also was from

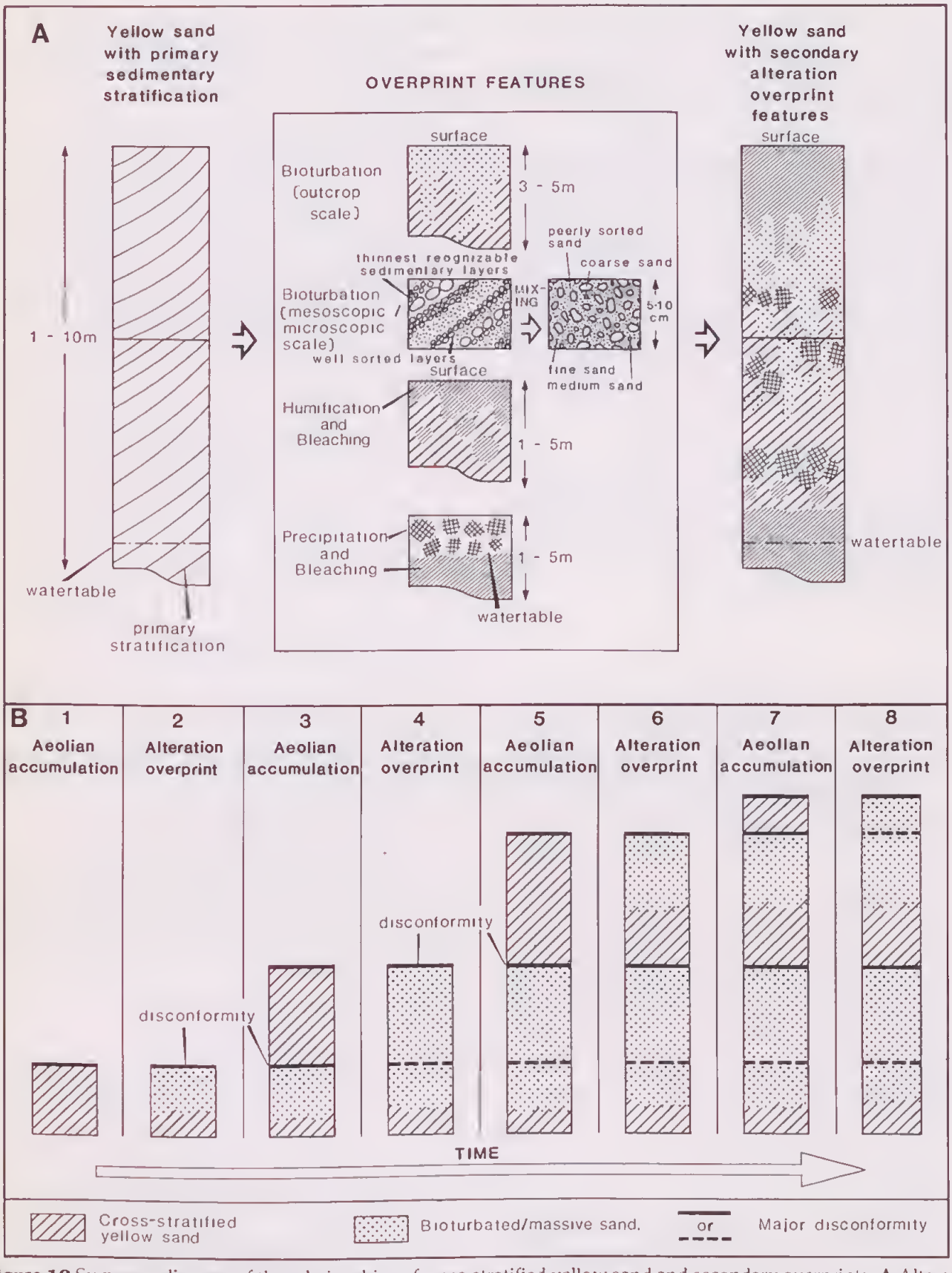

Figure 10 Summary diagram of the relationships of cross-stratified yellow sand and secondary overprints. **A** Alteration features which overprint and destroy primary cross-stratification. **B** Stages in the development of a multistoried sequence of intercalated cross-stratified sand, massive sand and major disconformities. For simplicity, zones of humification, cementation and bleaching are not shown.

the SW. An easterly wind direction for yellow sand emplacement is consistent with the occurrence of latest Pleistocene to Holocene lunette dunes, of the Swan Coastal Plain, which are located on the **western** sides of lakes (*eg* Benger Swamp, Forresdale Lake, White Lake; see Glassford 1980, Beard 1982).

The sequence of stratified units, representing major desert-aeolian phases or ergs, intercalated with the massive units beneath major disconformities suggest that the yellow sands of the Swan Coastal Plain record a mainly middle Pleistocene sequence of desert ergs. During Plio-Pleistocene times there have been more than 20 glacial periods (Kukla 1977, Lamb 1977, Hooghiemstra 1988) during which high latitude areas of the globe were extensively glaciated and sea levels were much lower than at present. The middle to low latitudes (such as the presently humid SW Australia) then were desertic with winds stronger than at present (Lamb 1977, Sarnthein 1978, Glassford 1980, Glennie 1987, Skackleton 1987, Rea & Leinen 1988). Additional desert-erg sequences may be preserved on the Yilgarn Block and possibly under the continental shelf of Western Australia (Glassford 1980, 1987).

Stratified yellow sands, bounded by major disconformities, thus record mainly middle Pleistocene glacial age desert phases, when desert ergs were developed on the exposed continental shelf and the ancestral Swan Coastal Plain. Glacial age desert-erg phases were separated by interglacial age semi-arid to humid phases, with their accompanying development of bioturbated palaeosols on disconformities.

Acknowledgements We thank M J Kriewaldt for critically reviewing the manuscript.

References

Allen A D 1981 Groundwater resources of the Swan Coastal Plain, near Perth, Western Australia. In: Groundwater resources of the Swan Coastal Plain (ed B R Whelan) CSIRO, 29-80.

Ahlbrandt T S & Fryberger S G 1981 Sedimentary features and significance of interdune deposits. In: Recent and ancient non-marine depositional environments: models for exploration (ed F G Ethridge & R M Flores) SEPM Spec Publ 31, Tulsa, Oklahoma, 293-314.

Ash J E & Wasson R J 1983 Vegetation and sand mobility in the Australian desert dunefield. Zeit Geomorph N F Suppl 45: 7-25

Bagnold R A 1941 The physics of Blown Sand and Desert Dunes. Methuen, London

Baxter J L 1977 Heavy mineral sand deposits of Western Australia. Geol Surv W Aust Min Res Bull 10

Beard J S 1982 Late Pleistocene aridity and aeolian landforms in Western Australia. In: Evolution of the flora and fauna of arid Australia (ed W R Barker & P J M Greenslade) Peacock Publ, Adelaide

Beard J S 1984 Aeolian landforms, Part 2. In: Beard J S & Springer B S Geographical data from the Vegetation Survey of Western Australia with map of aeolian landforms 1:3,000,000. Occ Paper 2, Vegmap Publ

Blakey R C, Peterson F & Kocurek G 1988 Synthesis of late Palaeozoic and Mesozoic eolian deposits of the Western Interior of the United States. Sediment Geol 56: 3-125.

Brindley G W & Brown G (eds) 1980 Crystal structures of clay minerals and their x-ray identification. Min Soc London

Brookfield M 1970 Dune trends and wind regime in central Australia. Zeit Geomorph Suppl 10: 121-153.

Brookfield M 1977 The origin of bounding surfaces in ancient aeolian sandstones. Sedimentology 24: 303-332.

Dept Conservation & Environment 1980 Atlas of natural resources Darling System Western Australia explanatory text. Univ W Aust Press, Nedlands.

Folk R L 1974 Petrology of sedimentary rocks. Hemphill, Austin, Texas.

Fryberger S G, Ahlbrandt T S & Andrews S 1979 Origin, sedimentary features and significance of low-angle eolian "sand sheet" deposits, great Sand Dunes National Monument and Vicinity, Colorado. J Sed Petrol 49: 733-746

Gary M, McAfee R & Wolf C L 1972 Glossary of geology. Am Geol Inst Washington D C.

Glassford D K 1980 Late Cainozoic desert eolian sedimentation in Western Australia. Ph D thesis, Univ W Aust.

Glassford D K 1987 Cainozoic stratigraphy of the Yeelirrie area, northeastern Yilgarn Block, Western Australia. J R Soc W Aust 70: 1-24.

Glassford D K & Killigrew L P 1976 Evidence for Quaternary westward extension of the Australian Desert into southwestern Australia. Search 7: 394-396

Glennie K W 1970 Desert sedimentary environments. Elsevier, Amsterdam.

Glennie K W 1987 Desert sedimentary environments, present and past - a summary. Sediment Geol 50: 135-165

Gozzard J R 1983 Fremantle Part Sheets 2033 I and 2033 IV, Perth Metropolitan Region, 1:50,000 Environmental Geology Series, Geol Surv W Aust.

Gozzard J R 1986 Perth, Sheet 2034 II and part 2034 III and 2134 III, Perth Metropolitan Region, 1:50,000 Environmental Geology Series, Geol Surv W Aust.

Hooghiemstra H 1988 The orbital-tuned marine oxygen isotope record applied to the middle and late Pleistocene pollen record of Funza (Colombian Andes). Palaeogeog Palaeoclim Palaeoecol 66: 9-17

Hunter R E 1977 Terminology of cross-stratified sedimentary layers and climbing ripple structures. J Sediment Petrol 47: 697-706.

Jopling A V 1978 Bedding genesis. In: The Encyclopaedia of Sedimentology (ed R W Fairbridge & J Bourgeois) Dowden, Hutchinson & Ross, Stousburg, Penn, 47-56.

Jordan J E 1986 Armadale, part sheets 2033 I and 2133 IV, Perth Metropolitan Region, 1:50,000 Environmental Geology Series, Geol Surv W Aust.

Killigrew L P & Glassford D K 1976 Origin and significance of kaolin spherites in sediments of southwestern Australia. Search 7: 393-394.

Klenowski G 1976 Geotechnical properties of the Coastal Limestone in the Perth Metropolitan area. Geol Surv W Aust Ann Rep for 1975: 42-46

Kocurek G 1981 Significance of interdune deposits and bounding surfaces in aeolian dune sands. Sedimentology 28: 753-780.

Kocurek G 1986 Origins of low-angle stratification in aeolian deposits. In: Aeolian Geomorphology (ed W G Nickling), 177-194. Allen & Unwin, London.

Kocurek G 1988 First-order and super bounding surfaces in eolian sequences - Bounding surfaces revisited. Sediment Geol 56: 193-206

Kukla G J 1977 Pleistocene land-sea correlations, I. Europe. Earth Sci Rev 13: 307-374

Lamb H H 1977 Climate present, past and future, volume 2, climatic history and the future. Metheun, London

Lancaster N 1988 The development of large aeolian bedforms. Sediment Geol 55: 69-89.

Leeder M R 1982 Sedimentology. Allen & Unwin, London.

Lindholm R C 1987 A practical approach to sedimentology. Allen & Unwin, London

Logan B W, Read J F & Davies G R 1970 History of carbonate sedimentation, Quaternary epoch, Shark Bay, Western Australia. Am Assoc Petrol Geol Mem 13: 38-84

Low G H 1971 Definition of two Quaternary formations in the Perth Basin. Geol Surv W Aust Ann Rep for 1970: 33-34.

Low G H & Lake R W 1970 Perth and environs geological maps, sheet 2: 1:50,000 scale. Geol Surv W Aust

Low G H, Lake R W, Baxter J L & Doepel J J G 1970 Perth and environs geological maps, sheet 3, 1:50,000 scale. Geol Surv W Aust

Lowry D C 1977 Perth Basin yellow sand. Search 8: 54-55.

Marzolf J E 1988 Controls on late Paleozoic and early Mesozoic eolian deposition of the Western United States. Sediment Geol 56: 167-191.

McArthur W M & Bettenay E 1960 The development and distribution of the soils of the Swan Coastal Plain, Western Australia. CSIRO Soil Publ 16.

McKee E D & Bigarella J J 1979 Sedimentary structures in dunes with two sections on the Lagoa dune field, Brazil. 83-136. In: Geol Surv Prof Paper 1052, US Gov Printing Office, Washington.

McKee E D & Tibbitts 1964 Primary structures of a seif dune and associated deposits in Libya. J Sediment Petrol 34: 5-17

McKee E D & Weir G W 1953 Terminology for stratification and cross-stratification in sedimentary rocks. Geol Soc Am Bull 64: 381-390.

Nemec W 1988 The shape of the rose. Sediment Geol 59 149-152.

Nielson J & Kocurek G 1987 Surface processes, deposits and development of star dunes: Dumont dune field, California. Geol Soc Am Bull 99: 177-186

Passmore J R 1970 Shallow coastal aquifers in the Rockingham district, Western Australia. Water Res Found Aust Bull 18: 83p

Pettijohn F J, Potter P E & Siever R 1987 Sand and sandstone, 2nd ed. Springer-Verlag, New York.

Playford P E, Cockbain A E & Low G H 1976 Geology of the Perth Basin Western Australia. Geol Surv W Aust Bull 124.

Playford P E, Cope R N, Cockbain A E, Low G H & Lowry D C 1975 Phanerozoic in Geology of Western Australia. W Aust Geol Surv Mem 2: 223-433.

Playford P E & Low G H 1972 Definitions of some new and revised rock units in the Perth Basin. Geol Surv W Aust Ann Rep for 1971: 44-46.

Potter P E & Pettijohn F J 1977 Paleocurrents and Basin analysis, 2nd ed. Springer-Verlag New York

Prider R T 1948 The geology of the Darling Scarp at Ridge Hill J R Soc W Aust 32. 105-129

Quilty P G 1974 Cainozoic stratigraphy in the Perth area. J R Soc W Aust 57: 16-31

Rea D K & Leinen M 1988 Asian aridity and the zonal westerlies: late Pleistocene and Holocene record of eolian deposition in the northwest Pacific Ocean Paleogeog Palaeoclim Palaeoecol 66: 1-8

Reiche P 1938 An analysis of cross-lamination, the Coconino Sandstone. J Geol 46 905-932.

Sarnthein M 1978 Sand deserts during glacial maximum (18,000 yBP) and climatic optimum (6,000 yBP) Nature 272. 43-46.

Searle D J & Semeniuk V 1985 The natural sectors of the inner Rottnest Shelf coast adjoining the Swan Coastal Plain. J R Soc W Aust 67: 116-136.

Semeniuk V 1983 The Quaternary history and geological history of the Australind-Leschenault Inlet area J R Soc W Aust 66: 71-83.

Semeniuk V & Glassford D K 1988 Significance of aeolian limestone lenses in quartz sand formations: an interdigitation of coastal and continental facies, Perth Basin, southwestern Australia. Sediment Geol 57: 199-209.

Shackleton N J 1987 Oxygen isotopes, ice volume and sea level. Quat Sci Rev 6: 183-190.

Talbot M R 1985 Major bounding surfaces in aeolian sandstones - a climatic model. Sediment 32: 257-265.

Thomas D S G & Goudie A S 1984 Ancient ergs of the Southern Hemisphere. In: Late Cainozoic palaeoclimates of the Southern Hemisphere (ed J C Vogel, N Basson, U Vogel & A Fuls) 407-418. Balkema, Rotterdam.

Ward J D 1988 Eolian, fluvial and pan (playa) facies of the Tertiary Tsondab Sandstone Formation in the central Namib Desert, Namibia. Sediment Geol 55: 143-162.

Wilde S A & Low G H 1978 Explanatory notes on the Perth 1:250,000 Geological Sheet, Western Australia Geol Surv W Aust.

Wilde S A & Low G H 1980 Explanatory notes on the Pinjarra 1:250,000 Geological Sheet, Western Australia. Geol Surv W Aust.

Wilson I G 1972 Aeolian bedforms - their development and origins. Sediment 19. 173-210.

Wyrwoll K H & King P D 1984 A criticism of the proposed regional extent of Late Cainozoic arid zone advances into south-western Australia. Catena 11: 273-288.

INSTRUCTIONS TO AUTHORS

The *Journal* publishes (after refereeing)

- papers dealing with original research done in Western Australia into any branch of the natural sciences;
- papers concerning some biological or geological aspect of Western Australia;
- authoritative overviews of any subject in the natural sciences, integrating research already largely published in the more specialized national or international journals, and interpreting such studies with the general membership of the Society in mind;
- analyses of controversial issues of great scientific moment in Western Australia.

Prospective authors of papers in the last two categories should consult the Hon Editor for further advice.

Contributions should be sent to **The Honorary Editor, Royal Society of Western Australia, Western Australian Museum, Francis Street, Perth, Western Australia, 6000.** Publication in the Society's *Journal* is available to all categories of members and to non-members residing outside Western Australia. Where all authors of a paper live in Western Australia at least one author must be a member of the Society. Papers by non-members living outside the State must be communicated through an Ordinary or an Honorary Member. Submission of a paper is taken to mean that the results have not been published or are not being considered for publication elsewhere. Free reprints are not provided. Reprints may be ordered at cost, provided that orders are submitted with the return book proofs. Authors are solely responsible for the accuracy of all information in their papers, and for any opinion they express.

Manuscripts. The original and two copies must be submitted. They should be typed on opaque white paper with double-spacing throughout and a 3 cm margin on the left-hand side. All pages should be numbered consecutively, including those carrying tables and captions to illustrations, which appear after the text. Illustrations, both line drawings and photographs, are to be numbered as figures in a common sequence, and each must be referred to in the text. In composite figures, made up of several photographs or diagrams, each of these should be designated by a letter (eg Figure 2B). To avoid risk of damage to original figures, authors may retain these until after the paper is accepted. The copies of the figures accompanying the manuscript must be of good quality.

Authors are advised to use the most recent issue of the *Journal* as a guide to the general format of their papers. Words to be placed in italics should be underlined. To facilitate editing, papers must be accompanied by a table of contents, on a separate sheet, showing the status of all headings.

Following acceptance and editing of the manuscript, authors with access to word processors/computers should amend their manuscript and forward to the Hon Editor their disk (noting the computer and word-processing program used) and one copy of the paper.

References must be set out as follows:

Paper Jackson A 1931 The Oligochaeta of South-Western Australia. J R Soc W Aust 17:17-136.

Twigg L, Majer J D & Kotula R 1983 The influence of fluoroacetate producing plants upon seed selection by seed harvesting ants. Mulga Res Centre W Aust Inst Technol, Bentley, Ann Rep 6:75-80.

Book Jacobs M R 1955 Growth Habits of the Eucalypts. For Timb Bur, Canberra.

Chapter in book Dell J 1983. The Importance of the Darling Scarp to Fauna. In: Scarp Symposium (ed J D Majer) W Aust Inst Technol, Bentley, 17-27.

The Title should begin with a keyword. The **Abstract** should not be an expanded title, but should include the main substance of the paper in a condensed form. The metric system (SI units) must be used. Taxonomic papers must follow the appropriate international Code of Nomenclature, and geological papers must adhere to the International Stratigraphic Guide. Spelling should follow the Concise Oxford Dictionary.

Authors should maintain a proper balance between length and substance, and papers longer than 10 000 words would need to be of exceptional importance to be considered for publication. Authors will be charged page costs (currently $30 per page) if papers exceed 8 printed pages. Short papers (2-4 printed pages) are particularly sought as these often ensure full use of the 32 pages available in each part.

Illustrations. These should be prepared to fit single or double column widths. Illustrations must include all necessary lettering, and be suitable for direct photographic reduction. No lettering should be smaller than 1 mm on reduction. To avoid unnecessary handling of the original illustrations, which are best prepared between 1.5 and 2 times the required size, authors are advised to supply extra prints already reduced. Additional printing costs, such as those for folding maps or colour blocks, will be charged to authors.

Supplementary Publications. Extensive sets of data, such as large tables or long appendices, may be classed as Supplementary Publications and not printed with the paper. Supplementary Publications will be lodged with the Society's Library (C/- Western Australian Museum, Perth, WA 6000) and with the National Library of Australia (Manuscript Section, Parkes Place, Barton, ACT 2600) and photocopies may be obtained from either institution upon payment of a fee.

VOLUME 72 (PART 3)

JOURNAL OF THE ROYAL SOCIETY OF WESTERN AUSTRALIA

CONTENTS VOLUME 72 PART 3 1990

Edited by I Abbott

Registered by Australia Post—Publication No. WBG 0351

No claim for non-receipt of the Journal will be entertained unless it is received within 12 months after publication of Part 4 of each Volume

The Royal Society of Western Australia, Western Australian Museum, Perth

The Journal of the Royal Society of Western Australia was founded in 1914. Its circulation exceeds 600 copies. Nearly 100 of these are distributed to institutions and societies elsewhere in Australia. A further 200 copies circulate to more than 40 countries. The Society also has over 350 personal members, most of whom are scientists working in Western Australia. The Journal is indexed and abstracted internationally.

A69349/6/89-700

GARRY L. DUFFIELD, Government Printer, Western Australia